Aus dem Institut für Anatomie II
der Heinrich-Heine-Universität Düsseldorf
Direktorin: Universitätsprofessorin Dr. phil. nat. Charlotte von Gall

Loss of Bmal1 impairs the glutamatergic light input to the SCN in mice

Dissertation

zur Erlangung des Grades eines Doktors der Medizin
der Medizinischen Fakultät der Heinrich-Heine-Universität Düsseldorf

vorgelegt von
Hüseyin Korkmaz
2025

Als Inauguraldissertation gedruckt mit der Genehmigung der Medizinischen Fakultät der Heinrich-Heine-Universität Düsseldorf

gez.:

Dekan: Univ. -Prof. Dr. med. Nikolaj-Klöckner

Erstgutachterin: Univ. -Prof. Dr. phil. nat. Charlotte von Gall

Zweitgutacher: Univ. -Prof. Dr. med. Rainer Guthoff

Ich widme diese Doktorarbeit meinen Eltern Yasemin und Mahsun Korkmaz
in Liebe und Dankbarkeit

All animal experiments were approved by the North-Rhine-Westphalia State Agency for Nature, Environment and Consumer Protection (LANUV), Germany (approval number: 84.02.04.2012 A102 and 84-02.04.2014 A314) and conform to international guidelines for the ethical use of experimental animals (Portaluppi et al., 2010).

Alle Tierversuche wurden von der Landesanstalt für Natur, Umwelt und Verbraucherschutz Nordrhein-Westfalen (LANUV), Deutschland, genehmigt (Genehmigungsnummern: 84.02.04.2012 A102 und 84-02.04.2014 A314) und entsprechen den internationalen Richtlinien für den ethischen Umgang mit Versuchstieren (Portaluppi et al., 2010).

Teile dieser Arbeit wurden veröffentlicht:
'Loss of Bmal1 impairs the glutamatergic light input to the SCN in mice.' *Frontiers in Cellular Neuroscience*, 27 February 2025, Section Cellular Neuropathology, Volume 19, 2025. https://doi.org/10.3389/fncel.2025.1538985

Zusammenfassung

Licht ist der stärkste Einflussfaktor für die Synchronisation rhythmischer Gehirn- und Körperfunktionen mit der Außenwelt, die im Wesentlichen vom zirkadianen System gesteuert werden. Die Lichtinformation wird in der Retina detektiert und über intrinsisch photosensitive retinale Ganglienzellen (ipRGCs) an den zentralen Taktgeber, den Nucleus suprachiasmaticus (SCN), übertragen. Dieser koordiniert untergeordnete Uhren im Gehirn und in der Peripherie. Auf zellulärer Ebene reguliert ein autoregulatorisches, molekulares Uhrwerk die rhythmische Zellfunktion. Ein Element dieses Uhrwerks ist das Basic-Helix-Loop-Helix ARNT-Like Protein 1 (Bmal1), welches an der Aufrechterhaltung der zellulären Homöostase beteiligt ist. Eine gezielte Deletion von Bmal1 führt zur Störung zirkadianer Rhythmen und somit zu pathologischen Veränderungen. Es gibt Hinweise darauf, dass die Verarbeitung von Lichtinformationen bei Bmal1-Knockout-Mäusen (Bmal1-/-) beeinträchtigt ist, der Mechanismus dahinter ist jedoch unklar. Ziel dieser Studie war es, die Rolle von Bmal1 in der glutamatergen Neurotransmission von Lichtsignalen von ipRGCs zum SCN bei erwachsenen männlichen Bmal1-/- und Wildtyp-Mäusen (Bmal1+/+) zu untersuchen. Wir analysierten die Auswirkungen der Bmal1-Deletion auf das lichtvermittelte Verhalten (Masking), die Netzhautmorphologie sowie die Immunreaktion der neuronalen Glutamat Transporter vGLUT1, vGLUT2 und des glialen Transporters GLAST in den retinalen Schichten und im SCN. Ebenso untersuchten wir die Immunreaktion von VIP im SCN. Es erfolgte eine postmortale Quantifizierung der Glutamat Konzentration im SCN. Mithilfe fokussierter Ionenstrahl-Scanning-Elektronenmikroskopie (FIB-SEM) und 3D-Rekonstruktion untersuchten wir die Ultrastruktur der Synapsen zwischen Retina und SCN. Unsere Ergebnisse zeigen, dass die Deletion von Bmal1 die Masking-Reaktion auf Licht beeinträchtigt. Die Dicke der retinalen Schichten sowie die Immunreaktion auf vGLUT1 und vGLUT2 waren bei Bma1-/- Mäusen verändert. Im SCN war die Immunreaktion auf vGLUT1, vGLUT2, GLAST und VIP verringert, während die Glutamat Konzentration erhöht war. Auf ultrastruktureller Ebene waren präsynaptische Endigungen vergrößert und der Abstand zwischen den synaptischen Vesikeln und des synaptischen Spalts erhöht, was auf eine Reduktion des sofort freisetzbaren Glutamat-Pools hinweist. Unsere Befunde zeigen, dass der Verlust von Bmal1 das lichtvermittelte Verhalten sowie die Morphologie und glutamaterge Signalübertragung in Retina und SCN beeinträchtigt. Die gestörte glutamaterge Signalübertragung an der tripartiten Synapse zwischen ipRGCs und VIP-exprimierenden Neuronen im SCN könnte zur Veränderung des lichtvermittelten Verhaltens beitragen. Eine gezielte Beeinflussung der molekularen Uhr, einschließlich Bmal1, könnte eine potenzielle therapeutische Strategie zur Modulation von erhöhter Exzitotoxizität infolge chronobiologischer Störungen darstellen.

Summary

Light is the strongest synchronizer of rhythmic brain and body functions, predominantly controlled by the circadian system, with the external environment. Light information is detected by the retina and transmitted via intrinsic photosensitive retinal ganglion cells (ipRGCs) to the central pacemaker of the circadian system: the suprachiasmatic nucleus (SCN), which in turn, coordinates the subordinate clocks in the brain and periphery. At the cellular level, there is an autoregulatory molecular clockwork that drives rhythmic cell function. The Basic Helix-Loop-Helix ARNT-Like Protein 1 (Bmal1) is an essential component of this molecular clock and is also involved in maintaining the cellular homeostasis. Loss of Bmal1 leads to disruption of circadian rhythms as well as drastic pathological changes. Data suggests that the processing of light information in Bmal1 knockout (Bmal1-/-) mice may be impaired, however, the underlying mechanism is still unclear. Thus, in this study, we aimed to investigate the role of Bmal1 in glutamatergic neurotransmission of light signals from ipRGCs to the SCN in adult male Bmal1-/- and wild-type (Bmal1+/+) mice. We investigated the effect of Bmal1 deletion on light-mediated behavior, retinal morphology as well as the immunoreaction of neuronal glutamate transporters vGLUT1,2 and glial glutamate transporter GLAST in the retinal layers and SCN in addition to the postmortem quantification of glutamate levels in the SCN. Using focused ion beam scanning electron microscopy (FIB-SEM) and 3D-reconstruction of synapses, we examined the ultrastructure of the synapses between the retina and SCN. The immunoreaction of VIP in the SCN was also assessed.

Our results show that the deletion of Bmal1 impairs masking response to light. The thickness of retinal layers and the immunoreaction of vGLUT1,2 were altered in Bmal1-/- mice. In the SCN, the immunoreaction to vGLUT1,2, GLAST, and VIP was decreased, while glutamate concentration was increased. At the ultrastructural level, presynaptic terminals were enlarged, and the distance between synaptic vesicles and the synaptic cleft was increased, indicating a reduction in glutamate readily releasable pool.

Our findings indicate that Bmal1 loss impairs light-mediated behavior, affects both morphology of and glutamatergic signaling within the retina and the SCN. The impairment of glutamatergic signaling at the tripartite synapse between the ipRGCs and VIP-expressing neurons in SCN may contribute to the alteration of light-mediated behavior. Thus, targeting the molecular clock, including Bmal1, could provide a novel therapeutic strategy for modulation of increased excitotoxicity through chronodisruption.

IV. List of abbreviations

ACTH - Adrenocorticotropic Hormone

AMPA - Alpha-Amino-3-Hydroxy-5-Methyl-4-Isoxazolepropionic Acid

ATP – Adenosine Triphosphate

AVP - Arginine Vasopressin

BMAL1 - Basic Helix-Loop-Helix ARNT-Like Protein 1

CCGs - Clock-Controlled Genes

CLOCK - Circadian Locomotor Output Cycles Kaput

CREB - cAMP Response Element-Binding Protein

CRH - Corticotropin-Releasing Hormone

CRY - Cryptochrome (Protein)

c-Fos – Fos Proto-Oncogene

DMH - Dorsomedial Hypothalamus

EAAT - Excitatory Amino Acid Transporter

EPSC - Excitatory Postsynaptic Current

EPSP - Excitatory Postsynaptic Potential

GABA - Gamma-Aminobutyric Acid

GAD - Glutamic Acid Decarboxylase

GLAST - Glutamate-Aspartate Transporter

GLT-1 - Glutamate Transporter 1

GnRH - Gonadotropin-Releasing Hormone

GRP - Gastrin-Releasing Peptide

ipRGCs - Intrinsically Photosensitive Retinal Ganglion Cells

KO – Knockout

LGN – Lateral Geniculate Nucleus

MAPK - Mitogen-Activated Protein Kinase

mRNA - Messenger Ribonucleic Acid

NMDA - N-Methyl-D-Aspartate

NPAS2 - Neuronal PAS Domain Protein 2

OPN - Oculomotor Nucleus

PACAP - Pituitary Adenylate Cyclase-Activating Polypeptide

Per - Period (Gene/Protein)

Per2 - Period Circadian Regulator 2

PHb – Perihabenular Nucleus

PVN - Paraventricular Nucleus

RGCs - Retinal Ganglion Cells

RHT - Retinohypothalamic Tract

RORa - Retinoic Acid Receptor-Related Orphan Receptor Alpha

ROS - Reactive Oxygen Species

ROMO1 - Reactive Oxygen Species Modulator 1

SCG - Superior Cervical Ganglion

SCN - Suprachiasmatic Nucleus

TRH - Thyrotropin-Releasing Hormone

TTFL - Transcription-Translation Feedback Loop

VGLUT - Vesicular Glutamate Transporter

VIP - Vasoactive Intestinal Peptide

VPAC - Vasoactive Intestinal Peptide Receptor

WT - Wild Type

ZT12 - Zeitgeber Time 12

Table of contents

1.Introduction

1.1. Circadian rhythms

An important mechanism traced back to prehistoric times are, circadian rhythms (circa = around, diem = day) that help organisms adapt to environmental changes such as the day-night cycle, by synchronizing physiological, metabolic, and behavioral processes with the anticipated needs (Silver and Kriegsfeld, 2014). Those rhythms are generated by internal time-keeping mechanisms, even without any external cues or Zeitgebers (time giver in German) (Korf and von Gall, 2013), that may slightly deviate from the exact 24-hour cycle, allowing for continuous adjustment of the internal time keeping system to the outside world (Vitaterna et al., 2001).

1.2. Light input to the suprachiasmatic nucleus (SCN)

Light is the strongest Zeitgeber for synchronizing the mammalian daily physiological and behavioral activities with the day/night cycle. Light signaling relies on light inputs from various retinal photoreceptors (Kumar et al., 2024). The commonly known photoreceptors including rods and cones are responsible for vision. Rods contain rhodopsin and are specialized to detect light at low intensity and thus, they are responsible for night vision. Cones, on the other hand, contain photopsins and are responsible for daylight and color vision. The activation of both types of photoreceptors initiates phototransduction and the signals are transmitted via the synaptic terminal to bipolar and horizontal cells and finally to the retinal ganglion cells (RGCs) within the retina (Fu and Yau, 2007). Composed of the axons of retinal ganglion cells, the optic nerve transmits visual information to the lateral geniculate nucleus (LGN) of the thalamus ,the midbrain, regions, to subcortical regions and the visual cortex, which processes extrinsic visual cues, the interpretation, tracking of visual objects and patterns (Dhande and Huberman, 2014, Hattar et al., 2002).

As light can still be detected in some blind individuals, who lack image formation, the existence of additional photoreceptive cells independently of rods and cones was hypothesized. Further research revealed a subset of RGCs that represent about 2%, within this cell type and is able to respond to light independently. This is the result of melanopsin, which is the photopigment, responsible for this intrinsic photosensitivity, thus called intrinsically photosensitive (ipRGCS) (LeGates et al., 2014).

In line with this, genetically modified mice missing rods and cones could demonstrate preserved light detection, circadian entrainment, and non-image-forming visual functions. However, all light responses were abolished in mice additionally lacking melanopsin, confirming the role of melanopsin-expressing ipRGCs in non-image-forming vision (Pickard and Sollars, 2012, Fu et al., 2005).

The ipRGCs can be classified into five distinct cell types (M1 to M5) with diverse dendritic morphology, axonal projections, genetic profile, electrophysiological properties and function. M1 cells show the highest intrinsic light sensitivity and have a higher depolarized resting membrane potential and a lower spike frequency. Compared to that, M2 cells have medium somata and large sparsely branched dendrites. In contrast to that's, M2 cells show smaller, transient light responses but have higher firing rate capacity, greater excitability, and higher input resistance, making them more responsive to small synaptic inputs compared to M1 cells. In comparison to that, M3 cells resemble M2 cells in soma size and dendritic complexity and distribution. Their light responses are moderate and show sustained depolarizations and firing in response to light. M4 cells have large soma and large radially branched dendritic trees, while M5 have small soma with uniformly bushy, highly branched dendritic arbors. M3–M5 exhibit increased electrophysiological heterogeneity suggesting a broader and more specialized functional involvement in both non-image-forming and pattern vision (Ecker et al., 2010, Schmidt et al., 2011a, Schmidt and Kofuji, 2009, Schmidt and Kofuji, 2011, Hu et al., 2013, Berson et al., 2010). In addition to the afferent input received directly through the ipRGCs themselves, these cells can also integrate signals from rods and cones with their own slower, melanopsin-driven responses (Schmidt et al., 2011b).

The axons of ipRGCs mainly create the retinohypothalamic tract (RHT), which extends from the retina to the hypothalamus SCN. Dense nerve fiber terminals primarily terminate at the ventrolateral part of the SCN, with fewer projections to the SCN dorsomedial part (Moore et al., 1995). These projections mediate photic signals that are important for the regulation of circadian functions, independent of image-forming vision (Hannibal et al., 2002, Hannibal, 2002). Importantly, some ipRGCs that are projecting to the SCN can mediate light-induced effects on hippocampal learning and cognition independently of the SCN's role as a circadian pacemaker (Fernandez et al., 2018).

Beyond the SCN, the axons of ipRGCs project to other regions such as the anterior hypothalamus, retrochiasmatic area, lateral hypothalamus, perifornical area, and certain thalamic nuclei. Additionally, some ipRGCs terminate on the perihabenular nucleus

(PHb), which in turn project to prefrontal cortex and, thus, play an important role in light-influenced emotional regulation. Some axonal collaterals also reach the intergeniculate leaflet (IGL) and pretectum (Mikkelsen and Vrang, 1994, Johnson et al., 1988, Fernandez et al., 2018, Pickard, 1985).

Those mammalian ipRGCs utilize glutamate and the neuropeptide PACAP (pituitary adenylyl cyclase-activating polypeptide) as neurotransmitters for mediating light signal to SCN (Hannibal et al., 1997). With exposure to light, glutamate is released from synaptic vesicles in the axon terminals of RHT (Castel et al., 1993). In the SCN, glutamate binds to NMDA receptors, triggering a cascade that causes Ca^{2+} to flux into the neurons and resulting in neuronal activation. Meanwhile, PACAP promotes cAMP production through PACAP-R1 receptors (Hannibal et al., 2002, Chen et al., 1999, Hannibal et al., 1997). This causes the p44/42 MAPK signaling pathway to be activated, leading to the phosphorylation of CREB (cAMP response element-binding protein), a transcription factor, and an increase of c-Fos, that is a marker of neuronal activity. It also promotes the expression of the clock gene Per1 and photic resetting of the molecular clock in SCN cells (von Gall, 2022).

Each of these neurotransmitters have their own specifics, whereas PACAP is more effective during the late subjective day (darkness), glutamate primarily signals light during the early night, modulating the clock's phase precisely (von Gall et al., 2002). PACAP enhances the conductance of L-type calcium channels in SCN neurons, to enhance the intracellular calcium response to glutamate, a synergistic interaction where PACAP amplifies glutamate-induced signaling within the circadian clock (Dziema and Obrietan, 2002).

The SCN gets indirect photic input from IGL via the geniculohypothalamic tract, which releases GABA and neuropeptide Y (NPY) (Biello et al., 1997). Alongside this, additional projections from the raphe nuclei deliver nonphotic input to the suprachiasmatic nucleus (SCN), through serotonin (5-HT) release (Korf and von Gall, 2013).

1.3. The circadian Pacemaker

The circadian system is hierarchically organized in mammals. The time information, principally the light cues, is transferred to the master clock in the SCN, which generates the central circadian rhythm and subsequently synchronizes the peripheral clocks (Korf and von Gall, 2013).

The SCN is a paired nucleus located bilaterally around the third ventricle dorsal to the optic chiasm, within the anterior hypothalamus (Moore, 1997). Each SCN consists of around 10,000 neurons in addition to glial cells (Silver and Kriegsfeld, 2014). The SCN can be further anatomically divided into a ventrolateral part, referred to as the core region and the dorsomedial part of the SCN, the so-called shell region.

Furthermore, the SCN has diverse neuronal populations that express various neuropeptides and neurotransmitters. Mainly, the vasoactive intestinal peptide (VIP)-containing neurons represent 24% of SCN neurons and are located mainly in the core region. Whereas the shell region contains predominantly the arginine vasopressin (AVP)-positive neurons (37% of SCN neurons) (Figure 1). Other neurons express calretinin, and gastrin releasing peptide (GRP), neurotensin (each 14% of SCN neurons), while encephalin-, somatostatin-, and substance P-containing neurons represent less than 5% of SCN neurons. In addition, almost all SCN neurons contain gamma-aminobutyric acid (GABA) as a neurotransmitter, which can mediate both inhibitory and excitatory effect (Reghunandanan, 2024).

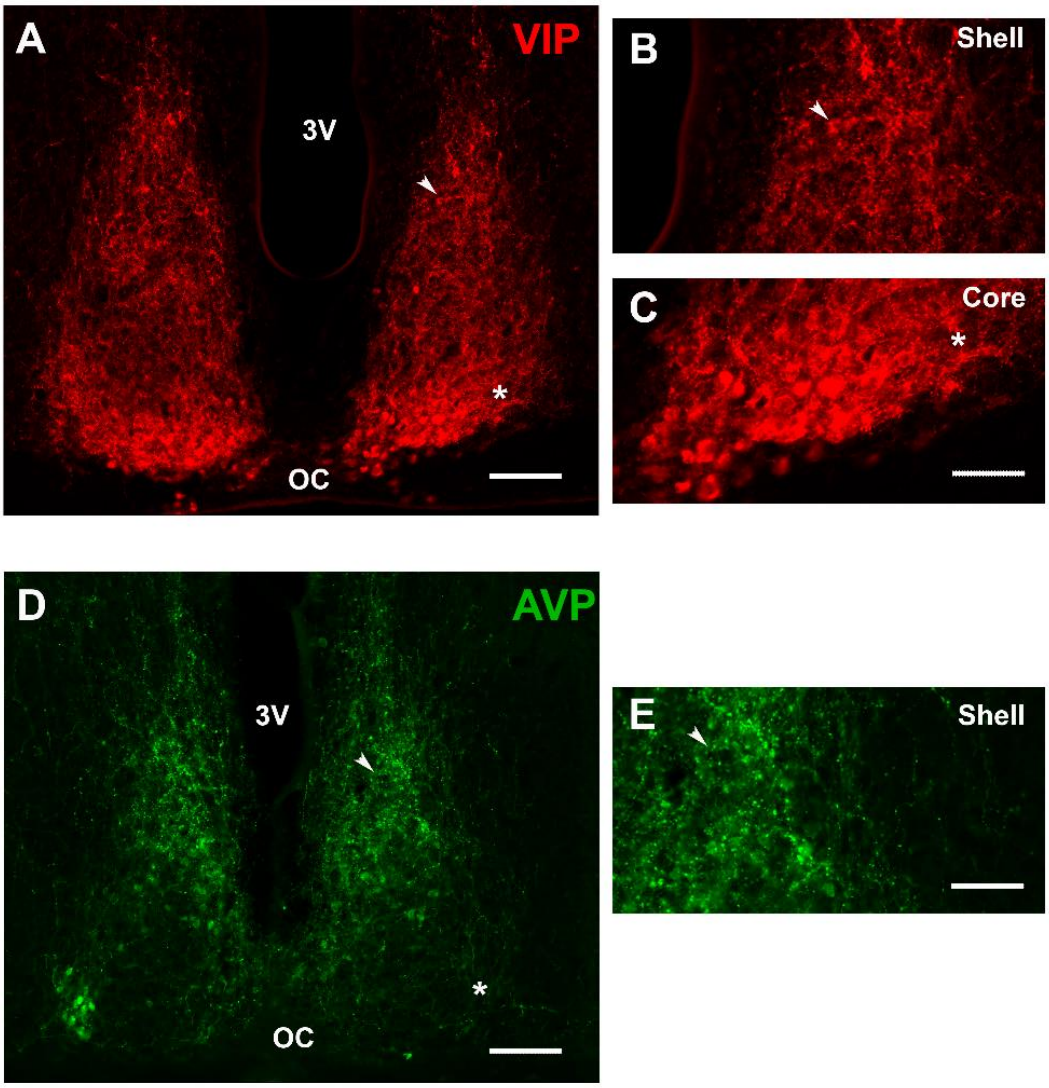

Figure 1: Immunoreactivity of key neuropeptides of the suprachiasmatic nucleus (SCN). Representative fluorescent image displaying (A Vasoactive intestinal peptide (VIP)-immunoreactivity (red) within the SCN. Higher magnification images show VIP-positive (B) axons (in the shell region) and (C) cell bodies (in the core region). Representative fluorescent images show (D) Arginine Vasopressin (AVP) immunoreactivity (green) in the SCN. High magnification images reveal (E) AVP-positive axons and cell bodies (in the shell region). The arrowhead marks the shell region, and the asterisk indicates the core region of the SCN. Scale bar = 100 µm in A, D. Scale bar = 50 µm in B, C, E. Reused with copyright permission under Creative Commons CC BY 4.0 license from (Yassine et al., 2024).

VIP- expressing neurons are the main light-recipient SCN neurons. Exposure to light increases the activity of VIP neurons in the SCN and enhances VIP release. VIP binds to its specific G-protein-coupled receptors, VPAC1,2 (Dickson and Finlayson, 2009), that are expressed in 60% of SCN neurons, leading to resetting by light and maintenance of coherent rhythmic firing within in the SCN neurons (Reghunandanan and Reghunandanan, 2006). The response of VIP neurons to light is stronger at dusk compared to other times of the day. However, prolonged exposure to constant light disrupts the circadian rhythm, causing VIP neuron activity to become arrhythmic (Dziema and Obrietan, 2002). Impaired VIPergic signaling upon loss of VIP or its receptor vasoactive intestinal peptide receptor 2 (VPAC2), a desynchronization of rhythmic neurons in the SCN is observed. So, these VIP-expressing neurons are the primary circadian pacemakers in the SCN and are crucial to establish and coordinating rhythms in other neurons and influencing behavioral patterns (Harmar et al., 2002, Aton et al., 2005)

VIP- expressing neurons are the main light-recipient SCN neurons. Exposure to light increases the activity of VIP neurons in the SCN and enhances VIP release. VIP binds to its specific G-protein-coupled receptors, VPAC1,2 (Dickson & Finlayson, 2009), that are expressed in 60% of SCN neurons, leading to resetting by light and maintenance of coherent rhythmic firing within in the SCN neurons (Reghunandanan & Reghunandanan, 2006). The response of VIP neurons to light is stronger at dusk compared to other times of the day. However, prolonged exposure to constant light disrupts the circadian rhythm, causing VIP neuron activity to become arrhythmic (Dziema & Obrietan, 2002). Impaired VIPergic signaling upon loss of VIP or its receptor VPAC2, a desynchronization of rhythmic neurons in the SCN is observed. So, these VIP-expressing neurons are the primary circadian pacemakers in the SCN and are crucial for establishing, coordinating rhythms in other neurons and influencing behavioral patterns (Aton et al., 2005, Harmar et al., 2002).

Conversly, AVP neurons are located in the SCN shell, show a robust circadian expression regulated by CLOCK/BMAL1 through E-box-mediated transcription. The synchronization of AVP is lower in comparison to VIP, but it plays a crucial role in regulating the coordination of the SCN network, that controls daily activity patterns, including the activity of organisms in the morning and the evening (Ono et al., 2021). Frankly, AVP neurons have also non-clock functions like promoting anticipatory thirst before sleep (Gizowski et al., 2016).

Other neurotransmitters such as, neurotensin, GRP, and GABA play a mediating function within the SCN network (Welsh et al., 2010, Reghunandanan, 2024) .

In addition to neurons, Astrocytes are crucial for brain health, regulating activity and rest through circadian rhythms. Disruptions, like impaired clocks in astrocytes, can lead to neurodegeneration or even cancer (Hastings et al., 2023).

.

1.4. SCN outputs

The Light information is transmitted from the SCN to the subordinate clocks in the central nervous system and the periphery via various outputs. The SCN's neuronal outputs target endocrine neurons containing Corticotropin-Releasing Hormone (CRH), Thyrotropin-Releasing Hormone (TRH) and Gonadotropin-Releasing Hormone (GnRH), neurons projecting to sympathetic or parasympathetic neurons in the spinal cord or brainstem and intermediate neurons processing information from the SCN and other hypothalamic centers and hence, regulate wide variety of physiological functions and behavior (Korf and von Gall, 2006).

For example, the SCN regulates the release of several hormones, like cortisol, via the hypothalamic-pituitary-adrenal (HPA) axis through both humoral factors and direct neuronal connections. AVP-expressing neurons within the SCN signal to the paraventricular nucleus of hypothalamus (PVN) and dorsomedial hypothalamus (DMH) (Kalsbeek et al., 2006).

Corticotropin-releasing hormone (CRH), is secreted by the hypothalamus, to be more specific, it is released from the parvocellular and magnocellular regions of the paraventricular nucleus (PVN), and the dorsomedial hypothalamic nucleus (DMH). These neurons stimulate the anterior pituitary to release adrenocorticotropic hormone (ACTH), which then acts on the adrenal cortex, that leads to the triggering of the production and release of cortisol. This hormonal cascade constitutes the core of the HPA axis and is tightly regulated by both circadian signals from the suprachiasmatic nucleus (SCN) (Tasker and Herman, 2011).

Additionally, indirect polysynaptic connections from preautonomic neurons in the PVN via the spinal cord and the autonomic nervous system contribute to regulating how responsive the adrenal cortex is to ACTH, ensuring that corticosterone production aligns with the circadian rhythm (Buijs et al., 2003). Glucocorticoids themselves feedback negatively on the HPA axis, acting on the hypothalamus and pituitary to regulate CRH

and ACTH secretion, thereby stabilizing the rhythm of cortisol output (Tasker and Herman, 2011).

As commonly known, the SCN controls the secretion of melatonin from the pineal gland through a complex, multisynaptic network. This pathway includes the PVN, preganglionic sympathetic neurons in the intermediolateral cell column of the spinal cord, and the superior cervical ganglion (SCG), which projects to the pineal gland. In darkness, the SCN has an effect on this circuit by reducing the inhibitory signaling to it, and also enhance the melatonin synthesis and release (Kalsbeek et al., 2006).

Besides promoting sleep, melatonin exerts inhibitory effects on the HPA axis, likely via melatonin receptors in the PVN and related hypothalamic structures, contributing to the suppression of cortisol levels during the night (Hardeland et al., 2015).

Thus, in human, the SCN enhances melatonin production at night to promote sleep, while induces the HPA axis, leading to higher cortisol levels in the early morning to mediate wakefulness and metabolism (Korf and von Gall, 2006).

Furthermore, the SCN outputs regulate also rhythmic feeding and metabolism. The efferent signaling via the SCN to the lateral hypothalamus (LH) regulate hunger and satiety, and projections to the subfornical organ (SFO) are regulating the water intake. These behaviors serve as non-photic zeitgebers (time cues) alongside light, helping to synchronize the SCN with the external environment (Kalsbeek et al., 2006). Moreover, SCN boosts insulin sensitivity in muscles to strengthen glucose uptake while stimulating the liver to produce more glucose, thereby reassuring stable energy levels (Kalsbeek et al., 2014).

Importantly, signals from the SCN to the medial preoptic area (MPO) of the hypothalamus control daily fluctuations in body temperature (Silver and Kriegsfeld, 2014).

Rhythms in behavior and locomotor activity are important aspects of the circadian system and the synchronization to the external environment mainly light/dark cycle (Figure 2).

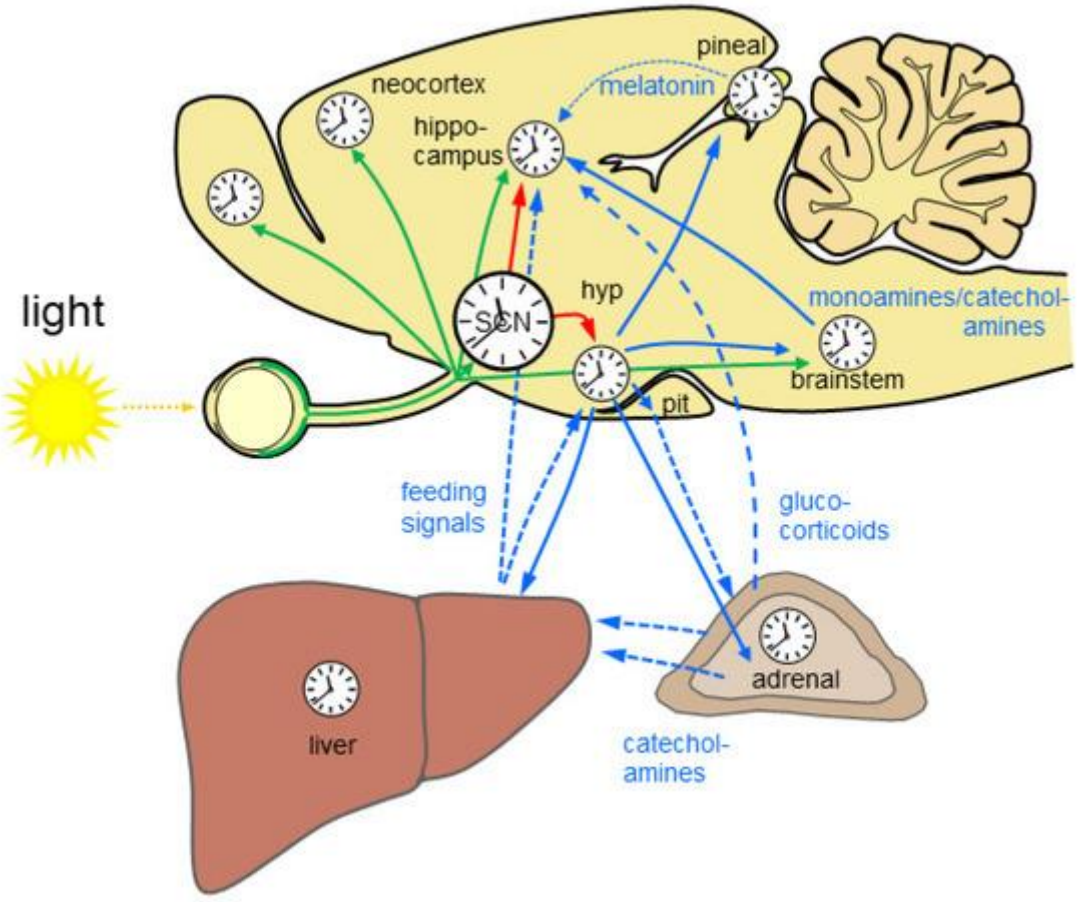

Figure 2: Hierarchy of the circadian system. The mammalian circadian system is a complex and hierarchically structured network. Nearly every brain region and organ contains its own molecular clock (clocks), which regulates rhythmic cellular activities. Light signals, both directly and indirectly, influence numerous brain areas (depicted by green arrows) and help establish time-of-day-dependent rhythms in the brain and body. The primary circadian rhythm generator is located in the suprachiasmatic nucleus (SCN) of the hypothalamus, and synchronized with exposure to light. If the SCN is damaged it leads to the disruption of circadian rhythms. The SCN's rhythmic output regulates secondary circadian oscillators in the brain (shown by red arrows). Various hypothalamic nuclei (hyp) manage rhythmic physiological processes and behaviors through neuronal pathways, including autonomic nervous system connections (solid blue arrows) and hormonal signals (dashed blue arrows) mediated by the pituitary gland (pit). The pineal gland and peripheral tissues also send rhythmic endocrine signals (blue dashed lines) that influence brain function. The liver is used as a representative example of the gastrointestinal system. Monoamines and catecholamines from the brainstem provide essential rhythmic drives that affect alertness and motivation in the forebrain. Reused with copyright permission under Creative Commons CC BY 4.0 license from (von Gall, 2022).

Two main mechanisms contribute to locomotor activity regulation in either a nocturnal or diurnal species (Mrosovsky, 1999).

The first mechanism, known as entrainment, in which the light signal is transmitted to the SCN to synchronize its period and phase with the environmental light-dark cycle. Given that the intrinsic circadian rhythm slightly deviates from a 24-hour cycle, regular adjustment is essential. The SCN enables anticipation of environmental light-dark changes and regulates activity in accordance to daily changes in light and darkness. Entrainment is an adaptive mechanism as the duration of the light and dark phases changes according to the seasons. Nocturnal mammals that live in dark burrows and only have environmental light conditions when they exit from their shelters are an example for this (von Gall, 2022).

Masking, is the second mechanism and describes how light can directly modulate behavior, bypassing regulation by the circadian system (Aschoff, 1960). In nocturnal species, this phenomenon is observed, where light can either suppress or promote activity depending on its brightness, so light can have two opposing effects on activity depending on the intensity of illumination. In low-light conditions, activity is increased compared to complete darkness. This boost in their activity, is named as positive masking, is believed to be influenced by enhanced confidence based on visual input (Thompson et al., 2008, Mrosovsky, 1999) . However, under bright light conditions, activity is suppressed even in the absence of visual cues, leading to decreased activity levels. This inhibitory effect of bright light on activity is known as negative masking (Mrosovsky, 1999). The exact brain region responsible for masking is still debatable, however, the intergeniculate leaflet (IGL) and retina–SCN projections are considered potential contributors (Morin, 1994, Fernandez et al., 2016, Morin, 2013).

1.5. Intracellular Molecular Clockwork

The circadian rhythms are driven by molecular clockwork that are present in almost every cell. The rhythmic gene expression is regulated by autoregulatory transcription/ translation feedback loops (TTLF) (Korf and von Gall, 2006).

The core clock components are composed of two stimulatory elements comprising the activating limb: Circadian Locomotor Output Cycles Kaput (Clock) and Basic helix-loop-helix ARNT-like protein 1 (Bmal1), and two inhibitory elements Period (Per1, 2) and Cryptochrome (Cry1, 2) constitute the inhibitory limb of the molecular clock machinery.

The transcription factors BMAL1 and CLOCK heterodimerize and bind to the promoter region, using E-box-like enhancer elements, resulting in the transcription of *Per* and *Cry* genes (Silver and Kriegsfeld, 2014). Subsequently, *Per* and *Cry* leave the nucleus and are translated into the cytosol. As a result, their protein products PER and CRY form a repressor molecule. The inhibitory complex created in the cytosol blocks the binding site of RNA polymerase, and the heterodimer Clock:Bmal1 is displaced from the promoter region, therefore leading to the inhibition of the transcription of *Per* and *Cry* (Reppert and Weaver, 2002).

The inhibitory complex is partially degraded by ubiquitination and disassembly within the proteasome, which results in the disinhibition of the negative feedback loop. Thus, the desinhibition of the BMAL1: CLOCK complex marks the beginning of a new cycle. This cycle lasts for around 24 hours, which leads to periodicity of gene and protein expression. The transcription of *Bmal1* can be further modulated by accessory feedback loops involving the orphan nuclear receptors ,Reverse Erythroblastosis Virus Alpha (REV-ERBα, gene: NR1D1), and Retinoic Acid Receptor-Related Orphan Receptor Alpha (RORa), which it inhibits or stimulates, respectively, the activity of Bmal1, by binding to the ROR-enhancer elements (Korf and von Gall, 2013) (Figure 3).

These cooperative and interlocking feedback loops ensure robustness against chronodisruption and maintain accurate circadian timing. Furthermore, they also generate phase delays in circadian transcriptional output, regulating gene expression to maintain temporal homeostasis with environmental cues (Partch et al., 2014).

PER1 is a crucial part of the negative feedback loop that controls the rhythmic expression of core clock and other multiple clock-controlled genes (CCGs). These CCGs regulate cellular activities that follow daily rhythms. In essence, the molecular clock coordinates the timing of gene expression to maintain rhythmic cellular function (Korf and von Gall, 2024).

Chronodisruption is the breakdown of internal 24-hour biological rhythms in synchrony with environmental cues, causing physiological disorder and promoting chronic health conditions (Erren and Reiter, 2009). Neurodegenerative diseases like Alzheimer's, Parkinson's, and Huntington's show early circadian disruption, which can worsen protein aggregation (mutant huntingtin in Huntington's, amyloid-ß and tau in Alzheimer's, and misfolded α-synuclein in Parkinson's), impair clearance mechanisms, and potentially accelerate disease progression (Colwell, 2021).

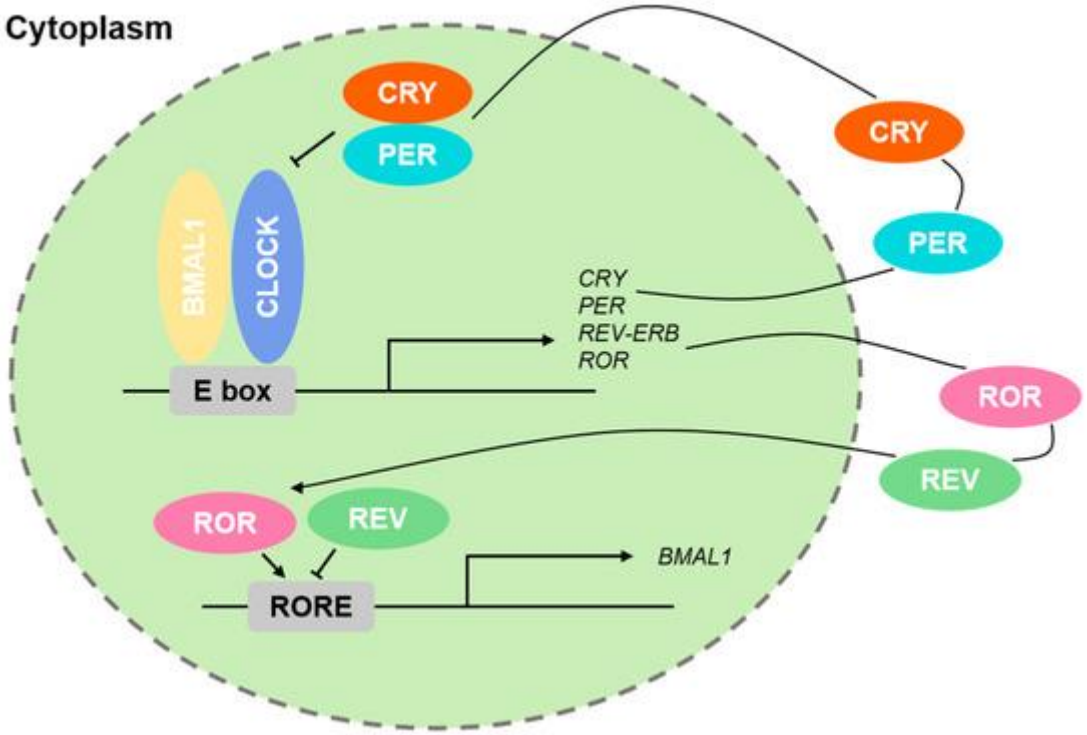

Figure 3: Intracellular molecular clockwork. The molecular circadian clock in mammals has two interlinked transcriptional-translational feedback loops. (1) In the core loop, Circadian Locomotor Output Cycles Kaput (CLOCK) and Basic Helix-Loop-Helix ARNT-Like Protein 1 (BMAL1) proteins activate the transcription of Period (Per) and Cryptochrome (Cry) genes. After that PER and CRY proteins form a complex that puts its effect on the nucleus and inhibit their own transcription by suppressing CLOCK-BMAL1 activity, maintaining a ~24-hour rhythm. (2) A stabilizing loop involves Retinoic Acid Receptor-Related Orphan Receptors (RORs) and Reverse erythroblastosis viruses (REV-ERBs), which compete for binding at the Bmal1 promoter. RORs act as activators, while REV-ERBs serve as repressors. Their opposing functions help regulate Bmal1 expression and stabilize the timing of the circadian cycle. Reused with copyright permission under Creative Commons CC BY 4.0 license from (Mao et al., 2025).

1.6. Bmal1-deficient mouse (Bmal1-/-)

The loss of Bmal1 disrupts circadian rhythms, particularly under constant darkness, and significantly reduces spontaneous locomotor activity in light-dark cycles (Bunger et al., 2000, Pfeffer et al., 2015). Bmal1-deficient mice originally created by Christopher Bradfield's show reduced negative masking response to light (Pfeffer et al., 2015, Pfeffer et al., 2009, Bunger et al., 2000). However, light-induced *Per* expression in SCN was particularly reduced in the early night phase in Bmal1-/- (Pfeffer et al., 2009). Additionally, the retinal-specific deletion of Bmal1 affects image processing (Baba et al.,

2018), suggesting a critical role for Bmal1 in transmitting light information from the retina to the brain. However, the specific involvement of Bmal1 in glutamatergic-mediated light signal transmission remains poorly understood.

In addition to loss of rhythmicity, mice with Bmal1 deletion have a shortened life expectancy, premature occurrence of age-related degenerative and pathological processes such as cataract and delayed wound healing. Furthermore, fewer osteoblasts and osteocytes are observed in Bmal1-/- mice, leading to age-related low bone mass, shorter bones, arthritis, and reduced bone density suggesting an important role in bone homeostasis and structure.

Moreover, Bmal1-/- displays an impaired adaptation to a novel environment, memory deficits and altered exploratory behavior (Samsa et al., 2016, Kondratov et al., 2006, Kondratova et al., 2010) associated with neuropathological changes, such as cellular senescence, premature astrogliosis and impaired neurogenesis. This may be attributed to disrupted control of neural precursor cells (NPCs) division (Bouchard-Cannon et al., 2013) as well as altered migration and differentiation potential of NPCs (Ali and von Gall, 2022, Ali et al., 2015). Additionally, even young Bmal1-/- mice show morphological changes in the perisynaptic fine astrocytic processes, indicating that the molecular clock plays a role in maintaining the integrity of the glial coverage at hippocampal tripartite synapse (Ali et al., 2020). Furthermore, Bmal1-knockout mice show age-dependent impairment of remyelination, which impacts the circadian-mediated functions such as sleep architecture (Rojo et al., 2022).

The pathological alteration may be closely related to elevated levels of reactive oxygen species (ROS) found in both brain and peripheral tissues of Bmal1-/- mice, indicating disrupted ROS homeostasis (Ali et al., 2015, Ali et al., 2020). This may be due to the accumulation of reactive oxygen species modulator 1 (ROMO1), which regulates intracellular ROS production, and elevated superoxide dismutase (SOD) concentrations (Silveira et al., 2020).

Another underlying mechanism of premature aging phenotype in Bmal1-deficient mice could be its impact on important cellular signaling pathways, for instance, the mechanistic Target of Rapamycin (mTOR) pathway, which is a key regulator of cellular growth, bone mineralization, hematopoiesis, hormone and neurotransmitter synthesis, metabolism, and proliferation. Furthermore, under normal conditions, there are Bmal1-dependent mechanisms that suppress mTOR signaling to limit anabolic activity and conserve resources. Thus, in Bmal1-/- mice, altered anabolism, which rapidly depletes nutrients

and energy, disrupts homeostasis, reduces physiological fitness and exhausts stem cell reserves, thus, ultimately resulting in accelerating aging in these animals (Khapre et al., 2014).

1.7. Glutamatergic signaling and concept of tripartite synapse

As the chief excitatory neurotransmitter in the mammalian central nervous system, glutamate plays a fundamental role in various brain processes like learning and memory. (Zhou and Danbolt, 2014). At the axon terminals of glutamatergic neurons, glutamate is packed into the synaptic vesicles via the vesicular glutamate transporters, which has three isoforms vGLUT1-3, via H^+-dependent ATPases (Omote et al., 2011). Both isoforms show a predominantly complementary expression pattern as vGLUT1 is expressed in cortex layers I–III and hippocampus while vGLUT2 is expressed in cortex layer IV, Thalamus and hypothalamus (Liguz-Lecznar and Skangiel-Kramska, 2007).

Although glutamate is the main neurotransmitter within the retina, vGLUT1 and vGLUT2 serve different functions. vGLUT1 mainly mediates the transmission of photoreceptor-evoked signals for image-forming vision (Johnson, 2007), while vGLUT2 is co-stored with PACAP in melanopsin-containing ipRGCs and involved in non-image forming function including circadian entrainment (Engelund et al., 2010).

Depolarization of the presynaptic terminals mediated by an intracellular Ca^{2+} increase leads to vesicle exocytosis of stored glutamate, which is then released into the synaptic cleft (Zhou and Danbolt, 2014). The released glutamate specifically binds to receptors on postsynaptic neurons. There are two types of glutamate receptor: 1. ionotropic receptors (iGluR) including AMPA, NMDA as well as kainate receptors and 2. metabotropic receptors (mGluR) (Reiner and Levitz, 2018). Glutamate binds to these receptors resulting in activating excitatory postsynaptic currents (EPSCs) (Hansen et al., 2021).

Importantly, astrocytes, together with the pre- and postsynapses, form the so-called tripartite synapse as a functional unit, which allows bidirectional communication between neurons and astrocytes (Farhy-Tselnicker and Allen, 2018). In addition, astrocytes regulates the integrity of glutamatergic synaptic transmission by astrocytic glutamate transporters including glutamate-aspartate transporter (GLAST). GLAST can take up glutamate from the synaptic cleft against and thereby prevent an excess of extracellular

excitatory glutamate, which could otherwise become neurotoxic (Šerý et al., 2015, Zhou and Danbolt, 2014).

The glutamate, which is rapidly taken up by astrocytes from the synaptic cleft, is reconverted within the astrocytes into glutamine by glutamine synthetase and transferred to the neurons where they are converted into glutamate by glutaminase and repackaged into synaptic vesicles (Figure 4). This glutamine–glutamate cycle plays a key role in maintaining the neuronal supply of glutamate (Hayashi, 2018).

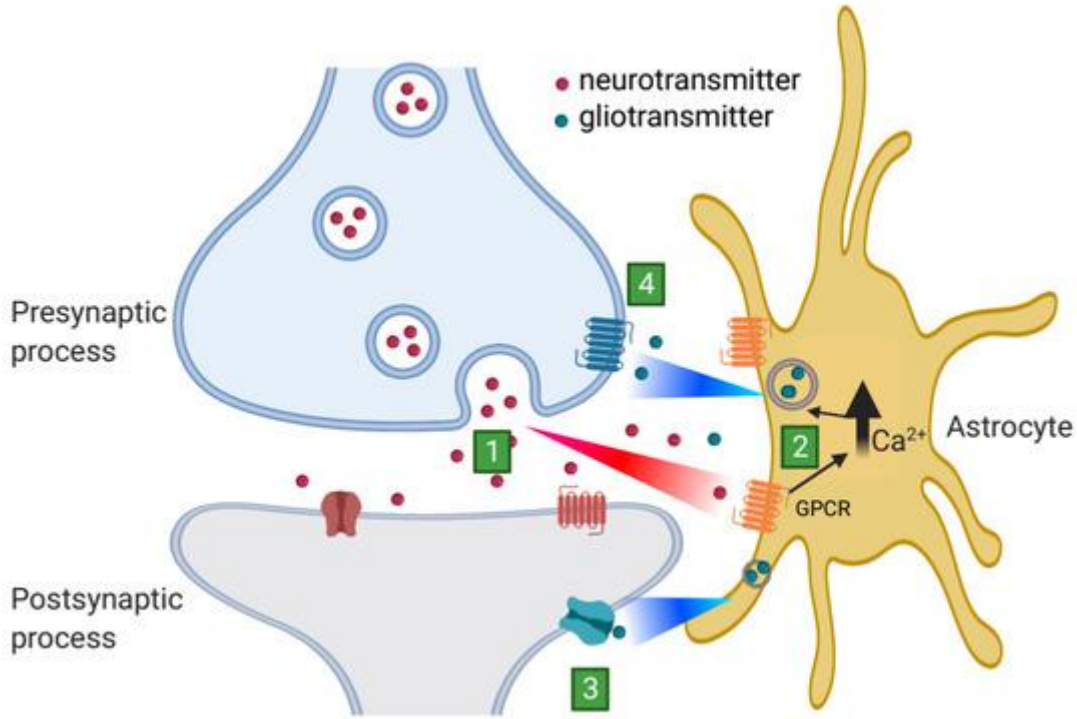

Figure 4: Structure of the tripartite synapse. A tripartite synapse is built of pre- and postsynaptic terminals surrounded by fine astrocytic processes. The action potential leads to the release of neurotransmitters from the presynaptic site that activate receptors on postsynaptic neurons and astrocytes. In astrocytes, this leads to a rise in intracellular calcium levels via G-protein coupled receptors signaling, which subsequently triggers the release of gliotransmitters. These gliotransmitters then modulate neuronal activity by acting on pre- or postsynaptic receptors. Reused with copyright permission under Creative Commons CC BY 4.0 license from (Nanclares et al., 2021).

2. Aim of the study

The aim of this study is to investigate the effect of Bmal1 loss on the glutamate-mediated transmission of light information from the retina to the suprachiasmatic nucleus (SCN). Specifically, we aimed to examine masking behavior in response to light, retinal morphology, and the immunoreaction of neuronal and astrocytic glutamate transporters in both the retina and SCN core region. Additionally, we assessed the ultrastructure of glutamatergic synapses between the retina and SCN. This study may also help elucidate the role of the molecular clock, particularly Bmal1, in the processing of non-image-forming light signals from the retina to the brain that may, in turn, impact various behavioral aspects, emotion and cognition. This can be particularly important in the treatment of neurological diseases associated with chronodisruption.

3. Original research article published from this work:

Loss of Bmal1 impairs the glutamatergic light input to the SCN in mice

Front. Cell. Neurosci., 27 February 2025
Sec. Cellular Neuropathology
Volume 19 - 2025 | https://doi.org/10.3389/fncel.2025.1538985

frontiers | Frontiers in Cellular Neuroscience

TYPE Original Research
PUBLISHED 27 February 2025
DOI 10.3389/fncel.2025.1538985

OPEN ACCESS

EDITED BY
Francisco M. Nadal-Nicolás,
National Eye Institute (NIH), United States

REVIEWED BY
Rongchen Huang,
University of Colorado, United States
Jens Hannibal,
University of Copenhagen, Denmark

*CORRESPONDENCE
Charlotte von Gall
✉ Charlotte.Gall@med.uni-duesseldorf.de

†These authors share last authorship

RECEIVED 03 December 2024
ACCEPTED 07 February 2025
PUBLISHED 27 February 2025

CITATION
Korkmaz H, Anstötz M, Wellinghof T, Fazari B, Hallenberger A, Bergmann AK, Niggetiedt E, Güven FD, Tundo-Lavalle F, Purath FFA, Bochinsky K, Gremer L, Willbold D, von Gall C and Ali AAH (2025) Loss of Bmal1 impairs the glutamatergic light input to the SCN in mice. *Front. Cell. Neurosci.* 19:1538985. doi: 10.3389/fncel.2025.1538985

Loss of Bmal1 impairs the glutamatergic light input to the SCN in mice

Hüseyin Korkmaz[1], Max Anstötz[1], Tim Wellinghof[1], Benedetta Fazari[1], Angelika Hallenberger[1], Ann Kathrin Bergmann[2], Elena Niggetiedt[1], Fatma Delâl Güven[1], Federica Tundo-Lavalle[1], Fathima Faiba A. Purath[1], Kevin Bochinsky[3], Lothar Gremer[3,4], Dieter Willbold[3,4], Charlotte von Gall[1*†] and Amira A. H. Ali[1,5,†]

[1]Faculty of Medicine, Institute of Anatomy II, Heinrich Heine University, Düsseldorf, Germany, [2]Core Facility for Electron Microscopy, Faculty of Medicine, Heinrich Heine University Düsseldorf, Düsseldorf, Germany, [3]Jülich Research Center, Institute of Biological Information Processing (IBI-7: Structural Biochemistry), Jülich, Germany, [4]Institute of Physical Biology, Heinrich-Heine-Universität Düsseldorf, Düsseldorf, Germany, [5]Department of Human Anatomy and Embryology, Faculty of Medicine, Mansoura University, Mansoura, Egypt

Introduction: Glutamate represents the dominant neurotransmitter that conveys the light information to the brain, including the suprachiasmatic nucleus (SCN), the central pacemaker for the circadian system. The neuronal and astrocytic glutamate transporters are crucial for maintaining efficient glutamatergic signaling. In the SCN, glutamatergic nerve terminals from the retina terminate on vasoactive intestinal polypeptide (VIP) neurons, which are essential for circadian functions. To date, little is known about the role of the core circadian clock gene, Bmal1, in glutamatergic neurotransmission of light signal to various brain regions.

Methods: The aim of this study was to further elucidate the role of Bmal1 in glutamatergic neurotransmission from the retina to the SCN. We therefore examined the spontaneous rhythmic locomotor activity, neuronal and glial glutamate transporters, as well as the ultrastructure of the synapse between the retinal ganglion cells (RGCs) and the SCN in adult male Bmal1−/− mice.

Results: We found that the deletion of Bmal1 affects the light-mediated behavior in mice, decreases the retinal thickness and affects the vesicular glutamate transporters (vGLUT1, 2) in the retina. Within the SCN, the immunoreaction of vGLUT1, 2, glial glutamate transporters (GLAST) and VIP was decreased while the glutamate concentration was elevated. At the ultrastructure level, the presynaptic terminals were enlarged and the distance between the synaptic vesicles and the synaptic cleft was increased, indicative of a decrease in the readily releasable pool at the excitatory synapses in Bmal1−/−.

Conclusion: Our data suggests that Bmal1 deletion affects the glutamate transmission in the retina and the SCN and affects the behavioral responses to light.

KEYWORDS

Bmal1, circadian system, SCN, vGLUT, GLAST, VIP, synapses

1 Introduction

In addition to its important function in image perception, light has a strong influence on a variety of brain functions. This includes the synchronization of rhythmic brain and body functions to the external time but also mood, emotions and cognition (Mahoney and Schmidt, 2024). Therefore, lighting conditions that deviate from the natural light-dark cycle can lead to chronodisruption and alter various brain functions (von Gall, 2022). On the other hand, chronodisruption might be linked to neurodegenerative diseases (Musiek and Holtzman, 2016). Rhythmic brain and body functions controlled by the circadian clock in the hypothalamic suprachiasmatic nucleus (SCN) can be entrained to rhythms in the environment such as the light-dark cycle. The light-dark cycle is also capable of modulating behavior and physiology independent of the circadian clock in a process called "masking" (Mrosovsky, 1999).

Intrinsically photosensitive retinal ganglion cells (ipRGCs), which contain the photopigment melanopsin, are essential for photic entrainment (Hattar et al., 2002; Panda et al., 2002; Ruby et al., 2002; Berson et al., 2002) and masking (Mrosovsky and Hattar, 2003) and mediate various other brain function responses to light, including alertness/sleep, mood/emotion and cognition (Lazzerini Ospri et al., 2024; LeGates et al., 2014; Zhang et al., 2021; Fernandez et al., 2018). A recent study by Lazzerini Ospri et al. (2024) highlights the importance of light mediated by the ipRGC for the integrity, activity and function of neural networks involved in the regulation of social, emotional and cognitive states. The SCN receives almost exclusively input from ipRGC (Beier et al., 2021) whose fibers form the retino-hypothalamic tract and mainly reach the vasoactive intestinal polypeptide (VIP)-containing neurons in the core region of the SCN (Kim et al., 2019). The VIP-containing SCN neurons are activated by light and are crucial for light entrainment (Jones et al., 2018; Todd et al., 2020). VIP also contributes significantly to maintain the circadian rhythm in the SCN at the cellular and network levels (Hamnett et al., 2019).

Glutamate represents the dominant neurotransmitter of the retina for image formation (Boccuni and Fairless, 2022) and non-image formation (Purrier et al., 2014). The neuropeptide pituitary adenylyl cyclase-activating peptide (PACAP) released as a co-transmitter by retinal ganglion cells, appears to be dispensable for masking by light (Colwell et al., 2004). The synaptic strength of synapses essentially depends on the synaptic vesicles. In glutamatergic synapses, the vesicular glutamate transporters vGLUT1 and vGLUT2 appear to be crucial not only for packing but also for vesicle trafficking and synaptic efficacy (Daniels et al., 2004; Engelund et al., 2010; Wojcik et al., 2004) with distinct synaptic release sites and in a non-overlapping complementary manner (Fremeau et al., 2001; Fremeau et al., 2004). Moreover, the glutamate transporters show a light-dependent oscillation in the brain which seems to be dependent on the molecular clockwork (Yelamanchili et al., 2006; Kiss et al., 2007; Darna et al., 2009; Chi-Castañeda and Ortega, 2018). In the SCN, the diurnal difference in the vGLUT1 and vGLUT2 immune response can be observed particularly in the area of the VIP neurons, which suggests a selective synaptic remodeling at sites of photic integration (Girardet et al., 2010). In addition, astrocytes contribute to the tripartite synapse with perisynaptic processes and regulate the extracellular glutamate level by both glutamate release and precise glutamate reuptake. The astrocytic glutamate aspartate transporter (GLAST) is essential for glutamate reuptake, thereby also preventing excitotoxicity (Todd and Hardingham, 2020), which is implicated in the pathogenesis of neurodegenerative diseases (Cuellar-Santoyo et al., 2023). Interestingly, VIP appears to be involved in preventing neurotoxicity in the brain by increasing glutamate reuptake (Brown, 2000), presumably through an increase in GLAST activity mediated by the VIP/VPAC2 receptor (Goursaud et al., 2008). Astrocytic glutamate reuptake and glutamine synthetase activity show daily rhythms (Leone et al., 2015). The astrocytic molecular clockwork appears to modulate GLAST and thereby the extracellular glutamate concentration (Beaulé et al., 2009; Cagampang et al., 1996; Spanagel et al., 2005). In the SCN, astrocytes contribute to the circadian timekeeping by modulating GABA- (Barca-Mayo et al., 2017) and glutamatergic-signaling (Chi-Castañeda and Ortega, 2018; Brancaccio et al., 2019).

Rhythmic cell function is controlled by a molecular clockwork which is composed of autoregulatory transcriptional/translational feedback loops of clock genes. The two transcription factors, Bmal1 and Clock are essential components of the molecular clockwork (Reppert and Weaver, 2002). In mice, Bmal1 deletion leads to a complete loss of circadian rhythmicity in constant darkness (Bunger et al., 2000) highlighting the importance of this clock gene for the circadian clock. Bmal1-deficient mice (Bmal1−/−) mice show a variety of pathological structural and functional changes throughout the body and brain as a result of accelerated aging, which is probably due to impaired redox homeostasis (Kondratov et al., 2006; Musiek et al., 2013; Ali et al., 2015). However, young Bmal1−/− mice also show morphological changes in perisynaptic astrocytic processes, suggesting a role of the molecular clockwork in the integrity of the tripartite synapse (Ali et al., 2020). Although Bmal1−/− mice show masking, their activity rhythm in the light-dark cycle is less robust than in their wild-type littermates (Pfeffer et al., 2015; Bunger et al., 2000) and the light-induction of clock genes is impaired (Pfeffer et al., 2009). Moreover, retina-specific deletion of Bmal1 affects visual image processing (Baba et al., 2018). These findings indicate an important role for Bmal1 in the transmission of light information from the retina to the brain. However, so far little is known about the role of Bmal1 in glutamatergic neurotransmission.

The aim of this study was to further elucidate the role of Bmal1 in glutamatergic neurotransmission from the retina to the brain. We therefore examined the neuronal and glial glutamate transporters as well as the ultrastructure of the synapse between the retina and the SCN, in adult Bmal1−/− mice. We focused on the SCN core region as an example because it represents the best characterized structure for ipRGC input. Our study contributes to a better understanding of the role of molecular clockwork in processing non-image-forming light information in the brain, which is also relevant in the context of changes in mood/emotions and cognition due to chronodisruption.

2 Material and methods

2.1 Experimental animals

Bmal1−/− and Bmal1+/+ littermates were obtained from breeding of Bmal1 heterozygous (Bmal1+/−) mice. Initial breeding pairs were obtained from Jackson Laboratories (B6.129-Arntltm1Bra/J). Adult male mice aged 4 months were used in this study (total: n = 19 Bmal1+/+, n = 20 Bmal1−/−). Mice were housed in standard cages in a temperature-controlled chamber (Beast Master, Germany) at the local animal facility of Düsseldorf University Hospital under 12-h light and 12-h darkness (lights on at 6:00 AM and off at 6:00 PM). The illumination (white light) intensity was 600 lx at the light phase and 0 lx during the dark phase. The mice had free access to food and water *ad libitum*.

All animal experiments were approved by the North Rhine-Westphalia State Agency for Nature, Environment and Consumer Protection (LANUV), Germany (approval number: 84.02.04.2012 A102 and 84-02.04.2014 A314) and conform to international guidelines for the ethical use of experimental animals (Portaluppi et al., 2010).

2.2 Monitoring of spontaneous locomotor activity

Bmal1−/− and Bmal1+/+ littermates (n = 6 mice per genotype) were housed individually in standard cages. Spontaneous locomotor activity was continuously recorded using on-cage infrared detectors (Mouse-E-Motion, Hamburg, Germany). The activity counts and the amplitude of the 24-h rhythm in spontaneous locomotor activity were analyzed using Clocklab software (Actimetrics, Wilmette, IL, USA) (Öztürk et al., 2021; Hassan et al., 2021). The percentage of activity counts during the day and the night to the total activity counts was calculated.

2.3 Immunohistochemistry

2.3.1 Tissue preparation

Mice (n = 5 mice per genotype) were sacrificed around the middle of the light phase (12: 00 pm = ZT06) by an overdose of ketamine/xylazine mixture (100 mg/kg or 10 mg/kg body weight, respectively), injected intraperitoneally. Mice were transcardially perfused with ice-cold 0.9% NaCl followed by 4% formalin in 0.1 M phosphate-buffered saline (PBS) using a Ministar Peristaltic Pump (World Precision Instruments, Sarasota, FL, USA). The eyes and the brains were carefully dissected, post-fixed in 4% formalin in PBS for 4 and 24 h, respectively. For cryoprotection, eyes and brains were stored subsequently in 20% and 30% sucrose for 24 h each and then embedded with optimum cutting temperature (OCT) compound. The eyes were cut into 14 μm thick sections along the anteroposterior axis, while the brains were cut into 20 μm thick coronal sections in the rostro-caudal extent of the SCN using a cryostat (Leica CM, Wetzlar, Germany).

For immunohistochemistry of whole-mount retina, mice (n = 4 mice per genotype) were killed using isoflurane. The eyes were dissected, fixed with 4% formalin for 15 min then washed with PBS. The anterior segment of the eye was removed, and the retina was separated from the sclera and the vitreous body. The retina was incised at the edges and dripped with cold methanol to smooth it out.

2.3.2 H&E staining

Retinal sections were rehydrated with Roticlear, followed by a descending alcohol series (100, 96, and 70%) and finally with distilled water. Then, the sections were stained with a Mayer's Hemalum solution (FA Merck 1.09249.1000) for 20 s and rinsed with 0.1% acid ethanol for 15 s followed by rinsing with tap water for 3–5 min. Sections were stained with Erythrosine B solution 0.1% aqueous for 1.5 min and rinsed again with distilled water for 30 s. Sections were dehydrated using increasing alcohol gradient (70, 96, and 100% EtOH) followed by Rothistol each twice for 5 min then cover-slipped using DEPEX.

2.3.3 Immunofluorescence

Slides with retinal and SCN sections were rinsed with 0.3% triton X-100 in PBS (PBST) and then incubated in 5% normal goat serum, in PBST and 0.25% BSA for 1 h at RT to quench unspecific antibody binding. Parallel retinal and brain sections were incubated with guinea pig anti-vGLUT1 (1:4000, Synaptic Systems, cat. #135304, Göttingen, Germany) or rabbit polyclonal anti-vGLUT2 antibody (1:3000, Synaptic Systems, cat. #135402 Göttingen, Germany). Additional parallel brain sections were incubated with rabbit polyclonal anti-VIP antibody (1:250, Acris/Peninsula Lab Burlington, MA, USA), rabbit polyclonal anti-EAAT1/GLAST-1 antibody (1:1000, ab416 Abcam Cambridge, Great Britain) or mouse monoclonal anti-GFAP antibody (1:500 BD-Pharmingen TM Material Number 556330, Franklin Lakes, New Jersey, USA) overnight at 4°C. Slides were then rinsed with PBST and subsequently incubated with the corresponding secondary antibodies: goat anti-mouse Alexa Fluor®568, goat anti-rabbit Alexa Fluor® 488, goat anti-rabbit Alexa Fluor® 568, goat anti-guinea pig Alexa Fluor® 488 (1:500, Molecular Probes, Eugene, OR, USA) for 1 h at RT. Slides were rinsed and then cover-slipped with the mounting medium (Fluoromount antifade, Southern Biotech). Retina whole-mounts were stained free floating using rabbit polyclonal anti-melanopsin (1:500, Clone UF008, cat#:1:AB-N39, Advanced Targeting Systems, San Diego, CA, USA) followed by goat anti-rabbit Alexa Fluor® 488 and cover slipped as mentioned above.

2.3.4 Image acquisition

Images of H&E-stained retinal sections were acquired in bright field mode using 40× objective. Z-stacks of immunofluorescence images of melanopsin-stained whole mount retina and single immunofluorescence images of VIP-stained SCN were acquired using a 20× objective of fluorescence microscope (KEYENCE BZ 900E, Keyence Corporation, Osaka, Japan), equipped with the respective fluorescence filters and lenses.

Single images of vGLUT1-, vGLUT2- and GLAST-immunofluorescence in the SCN were acquired using a confocal microscope (LSM SP8, Leica, Germany), equipped with high-resolution 63× NA 1.3 objective lenses Leica dye assistant was used and line sequential acquisition was selected. The following settings were used: format 1024×1024, zoom factor 4, a pinhole size of 1 Airy unit and a speed of 200. Confocal photomicrographs

were acquired from 3 independent fields within the SCN core region on both sides. The microscope acquisition settings were kept consistent in all samples for each staining set.

2.3.5 Image analysis

The genotype was obscured to the investigators. Image analysis of H&E staining and immunofluorescence images of retina and VIP was performed using the BZ-II analyzer software (Keyence Corporation, Osaka, Japan). Intact retinal sections devoid of histological artifacts were used. The width of the individual retinal layers at the midpoint between the optic disk and peripheral end of the retina was measured in three HE-stained retinal sections and averaged per animal. The Z-stacks of immunofluorescence images of melanopsin-stained whole mount retina were merged, the number of melanopsin positive retinal ganglion cells was counted manually in four independent fields in whole mount retina, which involves all retinal layers, and the density (cells/mm^2) was calculated. Background corrected fluorescence intensities in arbitrary units (a.u.) of the immunoreaction for the vesicular glutamate transporter (vGLUT1- and vGLUT2-Ir), GLAST-Ir and of VIP-Ir were analyzed in three parallel sections of each mouse and averaged. The background corrected fluorescence intensities (in a.u.) and the number of vGLUT1-, vGLUT2- and GLAST-positive particles were analyzed within the SCN core region using ImageJ software.[1] Only sections without artifacts or big blood vessels were included in the analysis. The particle analysis was performed in a defined area (46.18 μm × 46.18 μm) using macro including a median filter with a radius of 2 pixels, background subtraction using a rolling ball with a radius of 15 pixels, edges were enhanced using an unsharp mask (radius = 4, mask weight = 0.60) and threshold (38, 255). For particle separation, the image was converted to binary mask and the touching particles were separated by watershed.

2.4 Postmortem SCN neurochemistry

2.4.1 Tissue preparation and dual-phase metabolite extraction

Seven Bmal1+/+ and eight Bmal1−/− littermates were killed by cervical dislocation during the light phase (ZT6-ZT8). The brains were quickly dissected and cut into 1 mm thick sections in the coronal plane using an ice-cold mouse brain matrix. The SCN was bilaterally microdissected using a punch needle (15G), weighed and snap frozen. SCN tissue was homogenized in ice-cold double-distilled water (ddH_2O) and subjected to methanol/chloroform/water (1:1:1, v/v/v) dual-phase extraction as previously described (Koch et al., 2016). Briefly, 1 ml of ice-cold methanol was then added to the homogenized tissue, vortexed vigorously and incubated on ice for 15 min. Then 1 ml of ice-cold chloroform was added, vortexed and incubated for 10 min on ice. Finally, 800 μl of chilled ddH_2O were added, vortexed and incubated at 4°C overnight to enable phase separation. On the following day, the samples were centrifuged at 4,500 rpm for 25 min at 4°C. The upper phase containing the water-soluble metabolites was carefully separated. Lyophilization was then performed, and samples were stored at −80°C until measurement.

1 http://rsb.info.nih.gov/ij

2.4.2 Proton nuclear magnetic resonance (^{1}H-NMR) spectroscopy

Lyophilized tissue extracts obtained from dual phase metabolite extraction were resuspended in 210 μl 20 mM phosphate buffer (pH 7.0) containing 10% D_2O and 3-(Trimethylsilyl) propanoic acid (TSP; Lancaster Synthesis) as internal standard and transferred into 3 mm standard NMR tubes (Norell).

^{1}H NMR spectra of extracts were acquired on a 700 MHz (16.4 Tesla) Bruker AVANCE III HD 700 spectrometer equipped with a TCI 700S3 H-C/N-D-05 Z cryoprobe (Bruker). NMR data using 1-dimensional ^{1}H-experiments with excitation sculpting as water suppression were obtained with the following acquisition parameters: 25°C sample temperature, sweep width of 14 ppm, acquisition time 2 sec, relaxation delay 10 sec.

Metabolic glutamate determination was obtained by integration of ^{1}H NMR signals in the range of 2.3776–2.3386 ppm (Supplementary Figure 1A) characteristic for the CγH_2 moiety of glutamate and concentrations were calculated using the ERETIC2 concentration calculation tool from TopSpin (TopSpin software package, Vers. 3.6.4, Bruker). Glutamate standards were used as external standards and standard control measurements confirmed linearity of integrated signal intensity in the tested concentration range (glutamate concentrations of 95–526 μmol/L in the NMR test tube) (Supplementary Figure 1B).

2.5 Focused ion beam scanning electron microscopy

Mice (n = 3 per genotype) were killed by an overdose of ketamine/xylazine mixture as described in section "2.3.1 Tissue preparation." Mice were then transcardially perfused with 0.1 M phosphate buffer followed by the ice-cold 0.15 M cacodylate buffer with 2% formalin, 2.5% glutaraldehyde and 2 mM $CaCl_2$. Brains were dissected, post-fixed for 2 h at 4°C in the same fixative then rinsed using cacodylate buffer. Coronal brain sections of 150 μm thickness through the SCN between Bregma −1.5 and −2 (Paxinos and Franklin, 2012) were cut using a vibratome (VT1000S; Leica Microsystems GmbH, Wetzlar, Germany). Sections containing the mid-SCN level were selected from each mouse for further processing. Sections were rinsed with ice-cold 0.15 M cacodylate buffer containing 2 mM $CaCl_2$ and then incubated with cacodylate buffer containing 2% OsO_4 and 1.5% potassium ferrocyanide for 1 h. Sections were rinsed with ddH_2O and then incubated with 1% thiocarbohydrazide for 25 min at RT. Sections were rinsed with ddH_2O followed by incubation with 2% aqueous OsO_4 for 30 min at RT. After subsequent washing, sections were incubated with 1% aqueous uranyl acetate at 4°C overnight. Then, sections were rinsed and incubated with pre-warmed 0.02 M lead nitrate in 0.03 M aspartic acid, after adjusting the pH to 5.5, for 30 min at 60°C.

After washing with ddH_2O, sections were dehydrated in an ascending series of ethanol (30%, 50%, 60%, 70%, 90%, 95% to 100%) each 10 min followed by transferred to propylene oxide twice each for 2 min, then, to an ascending mixture of propylene oxide and epoxy resin (2:1, 1:1, 1:2) each for 1 h (Durcupan^{TM}; ACM, Fluka, Neu-Ulm, Germany). Finally, sections were transferred to pure epoxy resin and left overnight in RT. Then, sections were flat embedded in fresh epoxy resin within silicone rubber embedding

molds and the epoxy resin blocks were allowed to polymerize at 60°C for two days.

Epoxy resin blocks were trimmed around the tissue specimen containing SCN, semi-thin sections (100 nm) were cut on an ultramicrotome (Leica Ultracut UCT, Leica Microsystems GmbH, Wetzlar, Germany) and stained with Richardson's stain. The sample was attached to a sample stub using conductive silver paste (Cat# S066, Mikrotechnik Dr. Hert GmbH, Munich, Germany) and all the surfaces, except the surface to be imaged, were covered with silver paste to avoid charging of the epoxy-resin (Merchán-Pérez et al., 2009). The sample was left to dry overnight and then sputter-coated with a 20–24 nm thick layer of gold (108 auto, Cressington Scientific Instruments, Watford, UK).

Core region of SCN was identified by bright field microscopy as the area of interest and correlated with the optic image of the corresponding block surface in Focused Ion Beam Scanning Electron Microscope (FIB-SEM) (Crossbeam 550, Carl Zeiss AG, Oberkochen, Germany). FIB-SEM was used as it allows high resolution serial imaging simultaneously with sample surface removal using a focused gallium ion beam on a nanometer scale. The region of interest within core region of SCN was protected from undesired beam damage by a layer of platinum followed by a layer of carbon. This protective layer also contains tracking marks for automated image acquisition. Then, a trench, as a viewing channel, was coarsely milled using the FIB using 30 kV/15 nA ion beam current. The exposed cross section surface was further fine polished with the FIB using 30 kV/1.5 nA ion beam current.

The cross-section surface was serially milled using 30 kV/300 pA–30 kV/1.5 nA ion beam current depending on the sample and imaged with SEM perpendicular to the cutting plane using 2 kV acceleration voltage and an electron beam current of 69 pA with a frame time of 1 min 33 s per milling/imaging cycle. The backscattered electrons were detected by an InLens and an SE2 detector at a resolution of 2 nm/pixel and a slice thickness of 6 nm. A volume of 10 µm × 10 µm × 10 µm of dorsal SCN was imaged. The Atlas 5 software (Carl Zeiss AG, Oberkochen, Germany) was used for the collection of stacks of SEM images and automated correction of focus and alignment/astigmatism of serial micrographs. ImageJ software[1] was used for image pinning.

Six to seven presynaptic ends per animal were used for quantitative analysis. The presynaptic terminals were further classified based on the appearance of post synaptic density (PSD) into asymmetric synapses with a PSD thicker than the presynaptic membrane, while symmetric synapses have a similar PSD width to the presynaptic membrane. Asymmetric and symmetric synapses are correlated to excitatory or inhibitory synapses, respectively (Romaus-Sanjurjo et al., 2021). It has been previously shown that RHT synapses in the SCN contain both small clear core vesicles (glutamate-releasing) and dense core vesicles (PACAP-releasing) (Hannibal et al., 2000). Thus, only the excitatory presynaptic terminals containing both small clear core vesicles (40–60 nm in diameter) and larger dense core vesicles (80–100 nm in diameter), of asymmetric synapses in core region of SCN were included. The presynaptic terminal was delineated in serial images with a step size of 90 nm (15 image interval, each 6 nm). The surface area of the delineated presynaptic terminal and the area of synaptic contact were determined in each plane. The synaptic vesicles were counted in the labeled planes and their sum represented the number of vesicles in each presynaptic terminal. For each synapse, the density of synaptic vesicles per μm^2 was calculated and averaged for each animal. The volume of the presynaptic terminal was calculated by multiplying the measured presynaptic terminal area in subsequent planes by the step size. We further analyzed the mean distance of the synaptic vesicles to the synaptic cleft by averaging the minimal Euclidean distance of each vesicle to the associated reconstructed post synaptic density (PSD). This was used as an indicator of the readily releasable pool (RRP), defined as a subset of the vesicles in a presynaptic bouton that is more readily released than other vesicles and thus, closer to the presynaptic membrane. The reconstruction of vesicle positions and the PSD was performed in ImageJ. Subsequent calculation of the minimal Euclidean distances was performed in Microsoft Excel.

2.6 Statistical analysis

Statistical analysis was performed using Graph Pad Prism software. Values are presented as mean ± SEM. The normal distribution of the values within the groups of each data set was tested by Shapiro–Wilk test. When the values passed the normality test, parametric tests such as One-way ANOVA followed by Tukey's *post-hoc* test for multiple group comparisons or the Student *t*-test for comparison between two groups were applied. When the values were not normally distributed, non-parametric test, the Mann–Whitney-U test was applied. $p < 0.05$ was considered statistically significant.

3 Results

3.1 Bmal1 deficiency affects the rhythm in spontaneous locomotor activity under a light/dark cycle

The spontaneous locomotor activity was monitored under standard photoperiod of 12 h light/12 h darkness to study the response to light. The total activity count during a 24 h period was not significantly different between both groups. Both genotypes showed a higher activity during the dark phase than during the light phase (Figures 1A, B). However, Bmal1−/− mice showed a significantly lower activity during the dark phase and a significantly higher activity during the light phase compared to the Bmal1+/+ (Figure 1B). Moreover, the amplitude of the 24 h period was significantly lower in Bmal1−/− mice compared to Bmal1+/+ mice (Figure 1C). These findings indicate an impaired response to the light/dark cycle.

3.2 Bmal1 deficiency affects retinal morphology but not the number of ipRGCs

As the light information is received by the retina, we investigated the retinal architecture in HE-stained sections.

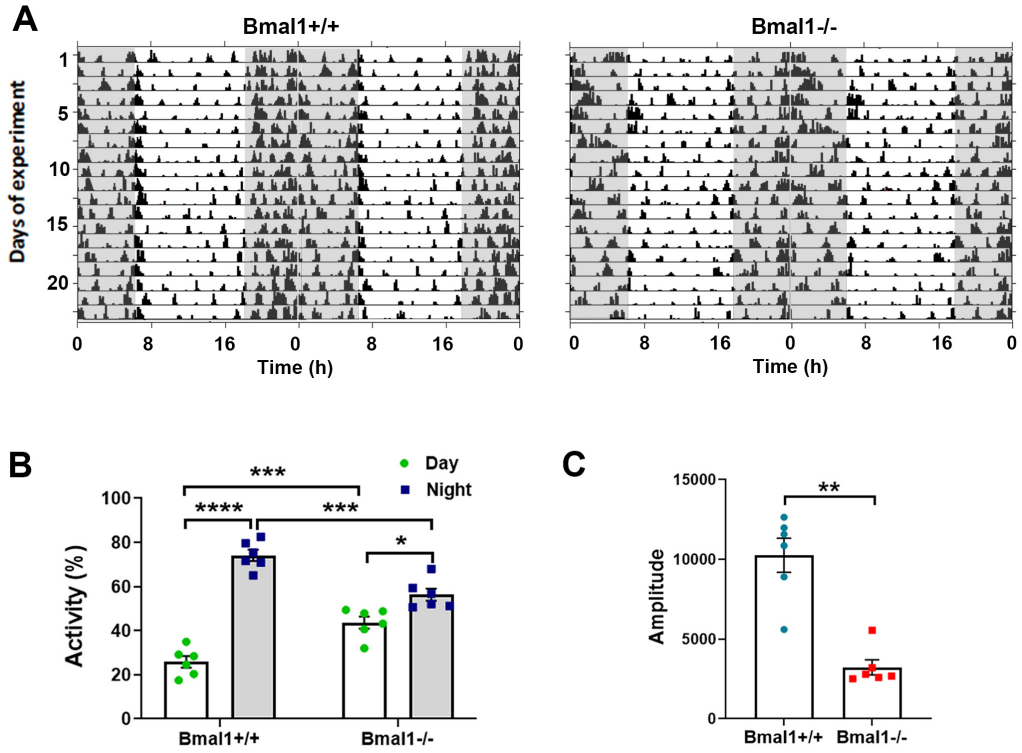

FIGURE 1
Bmal1 deficiency affects the rhythmic spontaneous locomotor activity. **(A)** Representative double plotted actograms of spontaneous locomotor activity of Bmal1+/+ and Bmal1−/− mice under a 12 h light/12 h dark cycle (LD). Gray-shaded boxes indicate periods of darkness. **(B)** Quantification of activity percentage during the light phase (white bars) and the dark phases (gray bars) to the total activity under the LD. One-way ANOVA test followed by Tukey's multiple comparisons test. **(C)** Amplitude of the 24 h rhythm in spontaneous locomotor activity. Mann–Whitney U-test. Values are shown as mean + SEM. *$p < 0.05$, **$p < 0.01$, ***$p < 0.001$. ****$p < 0.0001$. $n = 6$ mice per genotype.

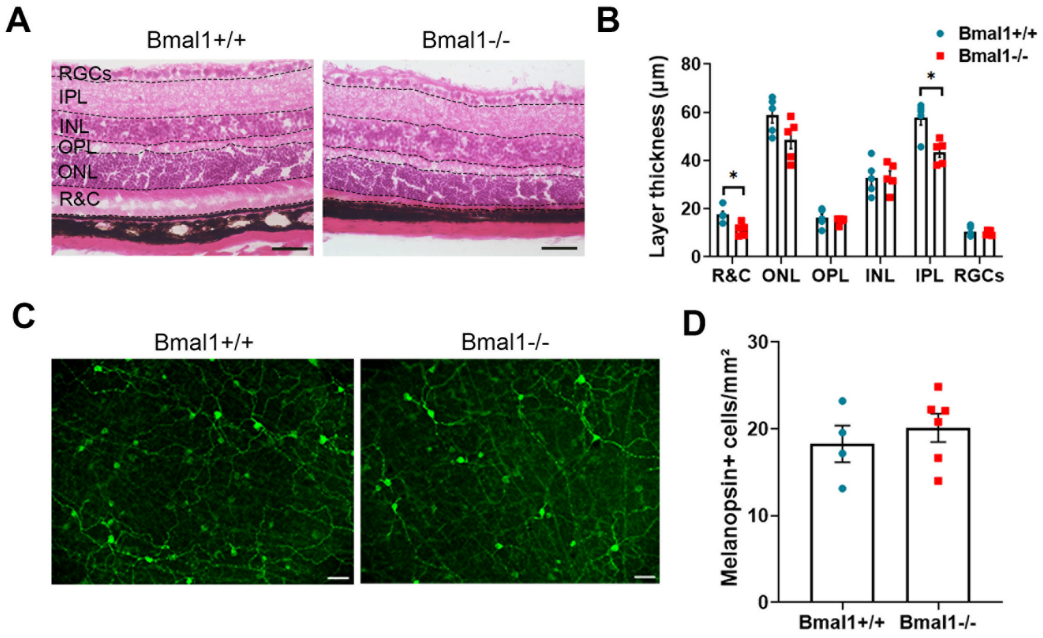

FIGURE 2
Bmal1 deficiency affects retinal morphology. **(A)** representative photomicrographs showing Hematoxylin and Eosin (HE)-stained retinal sections from Bmal1+/+ and Bmal1−/− mice. **(B)** Quantitative analysis of the thickness of retinal layers using Mann–Whitney-U-Test. R&C, rods and cones layer; ONL, outer nuclear layer; OPL, outer plexiform layer; INL, inner nuclear layer; IPL, inner plexiform layer; RGC, retinal ganglion cells. **(C)** Retinal whole-mounts showing melanopsin-immunoreactive cells (green) indicative for intrinsically photosensitive retinal ganglion cells (ipRGCs). **(D)** Quantification of the number of melanopsin positive (+) cells in the retina. Scale bars = 50 µm. Unpaired *t*-test, *$P < 0.05$.

Although retinal layering was preserved, the rods and cones layer as well as the inner plexiform layer were significantly thinner in Bmal1−/− mice than in wildtype littermates (Figures 2A, B). The number of melanopsin+ cells was not different between Bmal1+/+ (18.3 ± 2.1 cells/mm^2) and Bmal1−/− mice (20.1 ± 1.6 cells/mm^2) (Figures 2C, D). This indicates that the number of ipRGCs is not affected by Bmal1 deficiency.

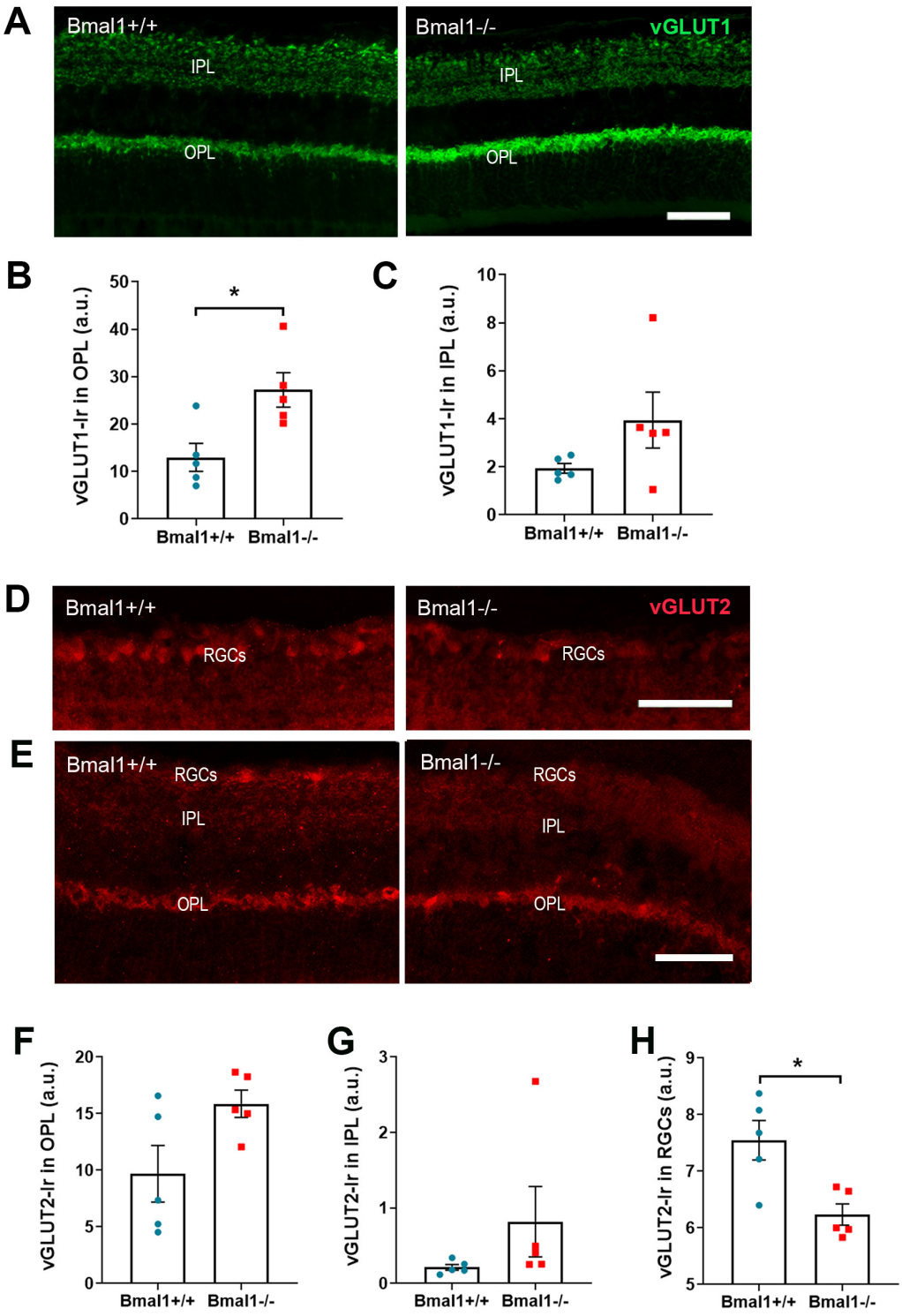

FIGURE 3
Bmal1 deficiency affects the vesicular glutamate transporters (vGLUT) in the retina. **(A)** Representative photomicrographs of vGLUT1-immunoreaction (green) in retinal sections of Bmal1+/+ and Bmal1−/− mice. Quantitative analysis of immunoreaction (Ir) of vGLUT1 in the **(B)** OPL and **(C)** IPL. **(D,E)** Representative photomicrographs of vGLUT2-Ir (red) in retinal sections from Bmal1+/+ and Bmal1−/− mice. Quantification of vGLUT2-Ir in the **(F)** OPL, **(G)** IPL and **(H)** RGCs. Scale bars = 50 μm. Unpaired-*t*-test, $*P < 0.05$.

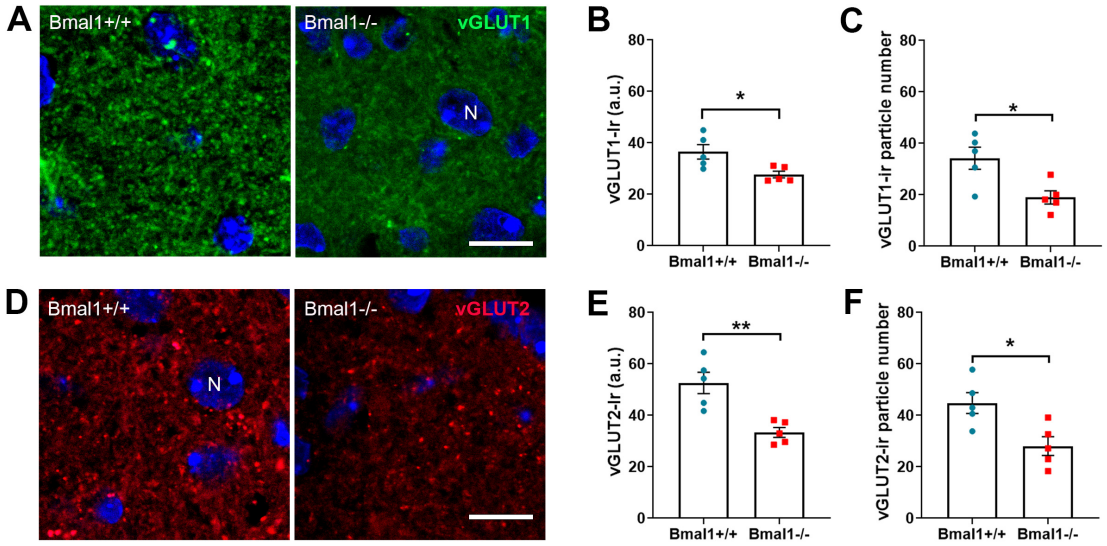

FIGURE 4
Bmal1 deficiency affects the vesicular glutamate transporters in the core region of the suprachiasmatic nucleus (SCN). **(A)** representative photomicrographs of vGLUT1-immunoreaction (green) in the SCN core region of Bmal1+/+ and Bmal1−/− mice. **(B)** Quantification of the fluorescent vGLUT1-immunoreaction (Ir) in arbitrary units (a.u.). **(C)** Number of vGLUT1-immunoreactive particles per SCN. **(D)** Representative photomicrographs of vGLUT2-Ir (red) in SCN core region of Bmal1+/+ and Bmal1−/− mice. **(E)** Quantification of fluorescent vGLUT2-Ir. **(F)** Quantification of the number of vGLUT2-immunoreactive particles. Immunoreactive particles were analyzed in a 46.18 μm^2 area. N, DAPI-stained cell nuclei (blue). Scale bars = 10 μm. Unpaired-*t*-test, $^*P < 0.05$, $^{**}P < 0.01$.

3.3 Bmal1 deficiency affects the vesicular glutamate transporters in the retina

Since glutamate is the predominant neurotransmitter in the retina, we analyzed the vesicular glutamate transporters, vGLUT1 and vGLUT2 in retinal layers.

vGLUT1-immunoreaction (Ir) was present in OPL and IPL (Figure 3A). In the OPL, vGLUT1-Ir was significantly lower in Bmal1+/+ mice than in Bmal1−/− mice (Figure 3B). In the IPL, vGLUT1-Ir was not significantly different between the genotypes (Figure 3C).

vGLUT2-Ir was present in IPL, OPL, and RGCs (Figures 3D, E). vGLUT2-Ir was not significantly different between the genotypes in the OPL (Figure 3F) and IPL (Figure 3G). However, in the RGCs, vGLUT2-Ir was significantly higher in Bmal1+/+ mice than in Bmal1−/− mice (Figure 3H). This indicates that Bmal1 deficiency alters the vGLUT1, 2 in retinal layers.

3.4 Bmal1 deficiency affects the vesicular glutamate transporter in the SCN core region

As glutamate is the main neurotransmitter that mediates light information from the retina to the brain, we exemplarily examined the vesicular glutamate transporters in the retinorecipient core region of the SCN.

In the core region of the SCN, vGLUT1-Ir was higher in Bmal1+/+ mice than in Bmal1−/− mice (Figures 4A–C). Similarly, vGLUT2-Ir was higher in Bmal1+/+ mice than in Bmal1−/− mice (Figures 4D–F), indicating that Bmal1 decreases the vGLUT1, 2 in SCN.

3.5 Bmal1 deficiency affects the ultrastructure of presynaptic terminals in SCN core region

Next, we analyzed the integrity of the presynaptic terminals in the SCN core region using Focused Ion Beam-Scanning Electron Microscopy (FIB-SEM).

In asymmetric, and therefore putative excitatory, synapses (Figure 5A), the number and the density of vesicles in the presynaptic terminals was not different between both genotypes (Figures 5B, C). However, in Bmal1−/− mice the size of presynaptic terminals (Figure 5D) as well as the distance of the vesicles to the synaptic cleft (Figure 5E) was larger compared to Bmal1+/+ mice.

In symmetric, and therefore putative inhibitory, synapses, there were no significant differences between the genotypes in the number and density of synaptic vesicles, in the size of the presynaptic terminals or in the distance of the vesicles to the synaptic cleft (Supplementary Figure 2). This data suggests that only excitatory, but not inhibitory synapses are altered in Bmal1−/− mice.

3.6 Bmal1 deficiency affects glutamate reuptake in the SCN

As the glial glutamate transporter GLAST is essential for the reuptake of glutamate from the synaptic cleft, we analyzed GLAST in the SCN core region. GLAST-Ir was significantly higher in Bmal1+/+ than in Bmal1−/− mice (Figures 6A–C). Moreover, the glutamate concentration was lower in SCN extracts from Bmal1+/+

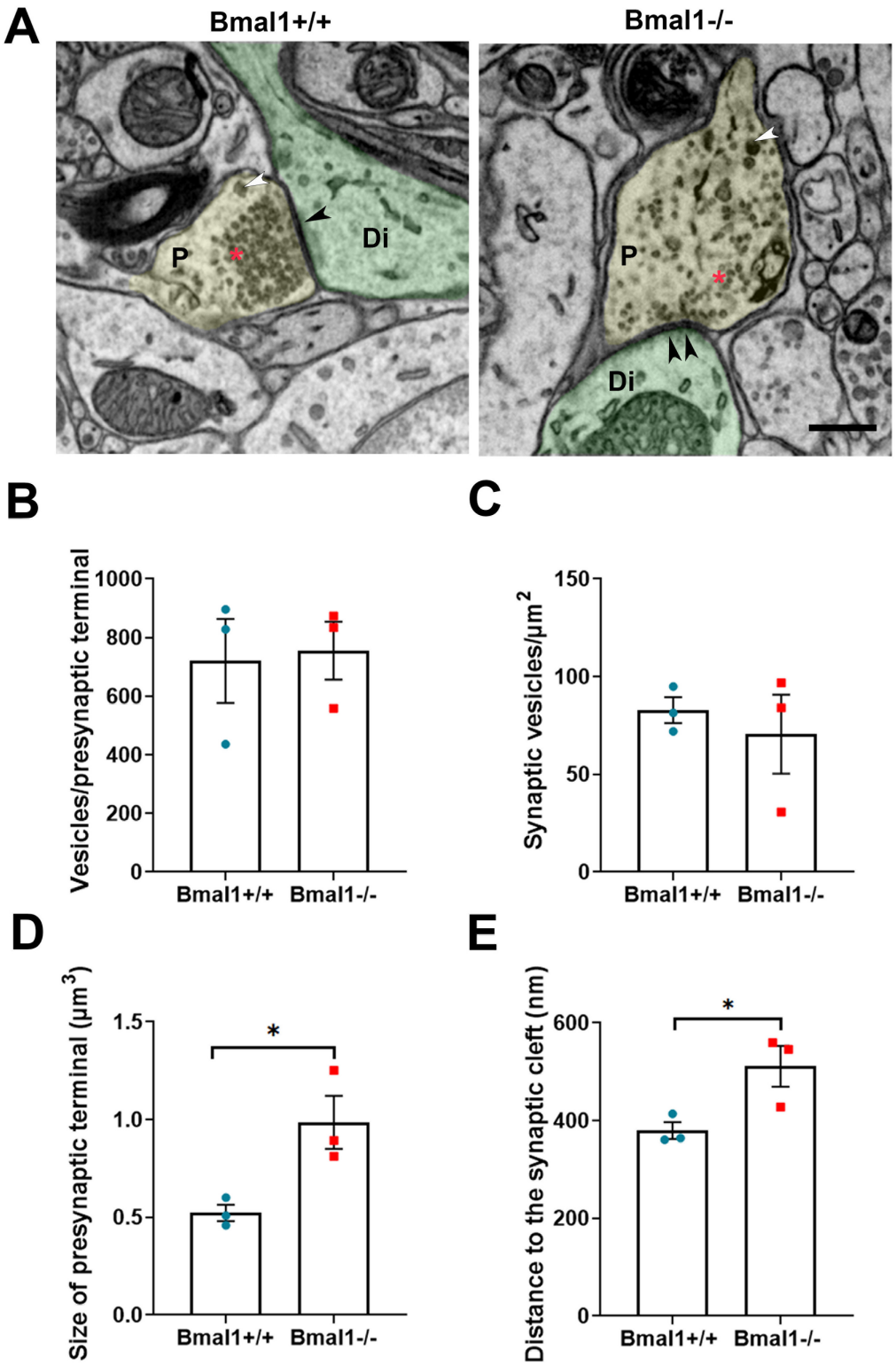

FIGURE 5
Bmal1 deficiency affects the ultrastructure of presynaptic terminals of the asymmetric/excitatory synapses in SCN core regions. **(A)** Representative electron micrographs showing presynaptic terminals (P, yellow), postsynaptic dendrites (Di, green) and synaptic density (black arrowhead) of asymmetrical synapses in SCN core region in Bmal1+/+ and Bmal1−/− mice. The red asterisk shows the small clear core vesicles; the white arrowhead shows the large dense core vesicles. Scale bar = 500 nm. **(B)** Quantification of the number of synaptic vesicles pro presynaptic terminal. **(C)** Quantification of synaptic vesicles density/μm^2 at the presynaptic terminal. **(D)** Quantification of the size of the presynaptic terminals in μm^3. **(E)** Quantification of the mean distance between the synaptic vesicles and the synaptic cleft in nm. Unpaired-*t*-test, $n = 3$ mice per genotype. *$P < 0.05$.

10.3389/fncel.2025.1538985

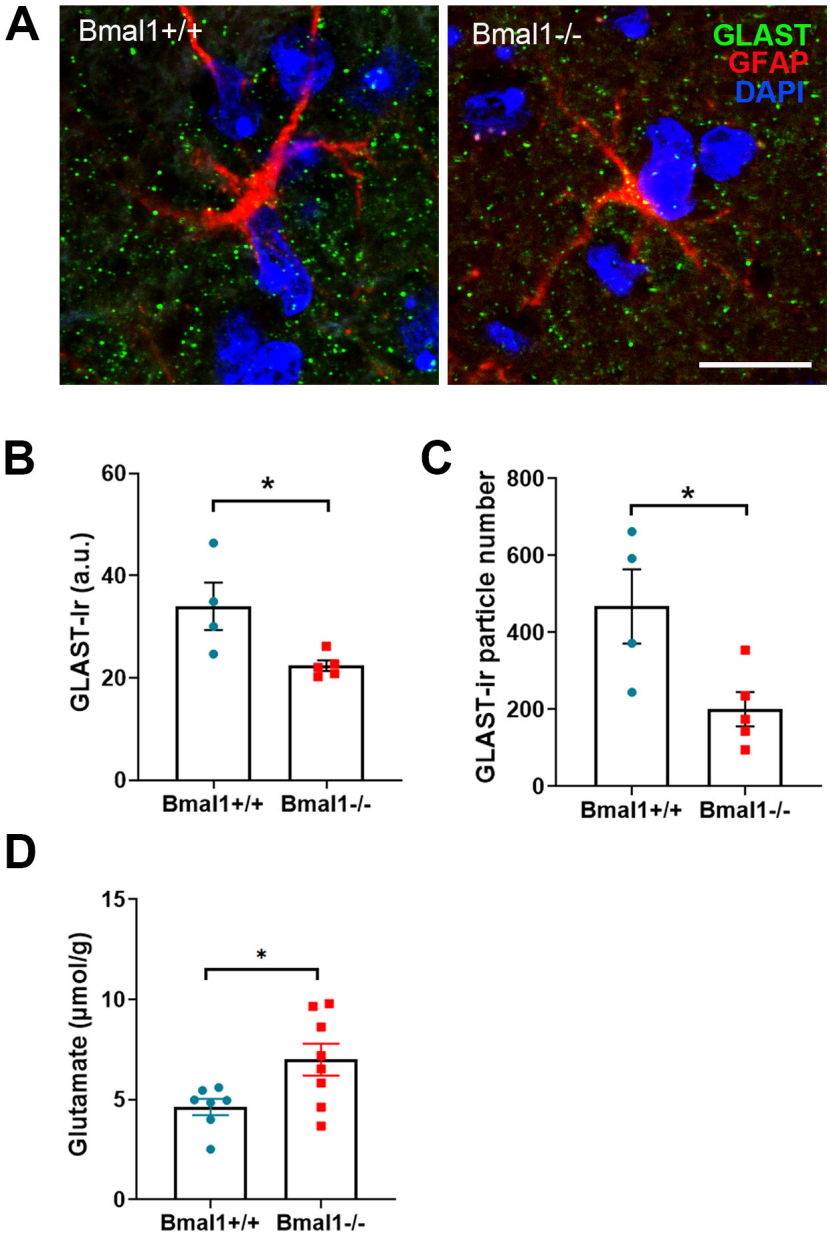

FIGURE 6
Bmal1 deficiency affects the glial glutamate transporter GLAST and glutamate levels in the suprachiasmatic nucleus (SCN). **(A)** representative photomicrographs showing immunoreaction of GLAST (green), astrocyte stem processes marker GFAP (red) and DAPI-stained nuclei (blue) in SCN core region in Bmal1+/+ and Bmal1−/− mice. Scale bar = 10 µm. **(B)** Quantification of immunoreaction (Ir) of GLAST in the SCN core in arbitrary unit (a.u.). **(C)** Quantification of the number of GLAST-Ir particles per SCN field (46.18 µm × 46.18 µm). **(D)** Quantification of postmortem glutamate concentration in the SCN. Unpaired-*t*-test, $*P < 0.05$.

than in those from Bmal1−/− mice (Figure 6D). These findings suggest an impaired glial reuptake of glutamate from the synaptic cleft in the SCN of Bmal1−/− mice.

3.7 Bmal1 deficiency affects the VIP+ neurons in the SCN core region

Finally, we analyzed the VIP neurons, which are the primary retinorecipient neuronal population of the glutamatergic retinal input to SCN. The immunoreaction of VIP was significantly decreased in the core region of SCN in Bmal1−/− compared to Bmal1+/+ ($P = 0.02$) (Figure 7). This suggests a lower activity of the retinorecipient neurons in the SCN.

4 Discussion

Signal transmission from the retina to the brain, which is glutamatergic, plays an important role not only in image formation but also in non-image-forming photic responses such as pupillary light response and acute suppression of locomotor activity by light

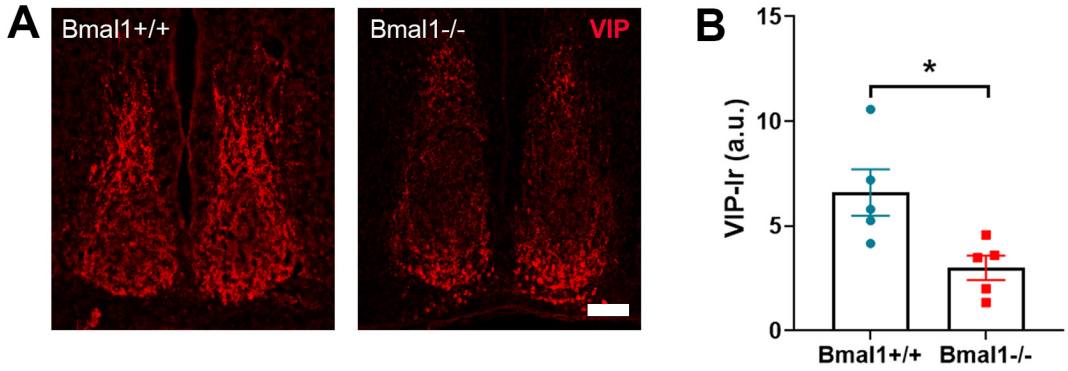

FIGURE 7
Bmal1 deficiency affects the vasoactive intestinal peptide (VIP) immunoreaction in the suprachiasmatic nucleus (SCN). **(A)** representative photomicrographs showing immunoreaction (Ir) of VIP (red) in SCN core region in Bmal1+/+ and Bmal1−/− mice. Scale bar = 100 μm. **(B)** Quantification of the VIP-Ir in the SCN. Unpaired-*t*-test. *$P < 0.05$.

(Hattar et al., 2002; Panda et al., 2002; Ruby et al., 2002; Berson et al., 2002; Panda et al., 2003; Mrosovsky and Hattar, 2003) as well as in mood, emotion and cognition (Lazzerini Ospri et al., 2024; Fernandez et al., 2018) . There is evidence that the clock gene Bmal1 is required not only for the generation of circadian rhythms (Bunger et al., 2000) but also for behavioral and molecular responses to light (Pfeffer et al., 2015; Bunger et al., 2000; Yang et al., 2019; Pfeffer et al., 2009) as well as visual image processing (Baba et al., 2018). In this study, we investigate how Bmal1 deficiency affects neuronal and glial glutamate transporters as well as the ultrastructure of the retina-SCN synapse. A better understanding of the role of the molecular clockwork in light transmission to the brain could also help better understand the alteration in brain function in response to chronodisruption.

Consistent with earlier studies (Pfeffer et al., 2015; Bunger et al., 2000), Bmal1−/− mice showed an impaired response of locomotor activity to the light-dark cycle. Consistent with a study on retina-specific deletion of Bmal1 (Baba et al., 2018), Bmal1−/− mice showed a thinner retina. However, the number of melanopsin-positive cells, representing the ipRGCs which are essential for non-image-forming photic responses (Hattar et al., 2002; Panda et al., 2002; Ruby et al., 2002; Berson et al., 2002; Panda et al., 2003; Mrosovsky and Hattar, 2003; Fernandez et al., 2018; Lazzerini Ospri et al., 2024), was not affected in Bmal1−/− mice. Therefore, it is unlikely that the impaired non-image-forming photic responses are due to morphological changes in the retina. However, immunoreaction of vGLUTs, which are essential for glutamatergic signaling (Engelund et al., 2010), in the retina was altered by Bmal1-deficiency. vGLUT1, which is essential for transmitting visual signals from rods and cones to bipolar and RGCs but dispensable for non-image-forming responses (Johnson et al., 2007) was upregulated in the OPL of Bmal1−/− mice. This may be a compensatory upregulation in response to thinning of the photoreceptor layer. Alternatively, it might be a consequence of the loss of retinal circadian clock function reported earlier in a retina-specific deletion of Bmal1 (Storch et al., 2007) because if the molecular clockwork is defective, the light-dependent fluctuation of vGLUT1 in the brain is abolished and shows a constantly high level (Yelamanchili et al., 2006). In contrast, vGLUT2, which is essential for non-image-forming responses to light (Gompf et al., 2015; Purrier et al., 2014; Land et al., 2004), was decreased in the RGC layer of Bmal1-deficient mice. Therefore, altered glutamatergic signaling from the bipolar cells to the RGCs could contribute to the attenuated non-image-forming photic responses of Bmal1−/− mice.

The ipRGCs transmit light information to a wide variety of subcortical and cortical brain regions. Among the subcortical regions that receive strong innervation from ipRGCs, the SCN is the most studied. Therefore, we examined the influence of Bmal1 deletion on the glutamate transporters in the SCN. Both vGLUT1 and vGLUT2 were detectable in the SCN, with vGLUT2-Ir being stronger, consistent with vGLUT2 being the preferred subtype in the ipRGCs (Engelund et al., 2010). In Bmal1−/− mice, both vGLUT1- and vGLUT2-Ir was reduced, supporting the hypothesis that the molecular clockwork plays a role in the control of glutamate transporters and thus glutamatergic synaptic efficacy (Darna et al., 2009; Chi-Castañeda and Ortega, 2018; Kiss et al., 2007; Yelamanchili et al., 2006).

We analyzed integrity of the synapses in the retino-recipient core SCN region at the ultrastructural level. There was no difference in the symmetric, and therefore putative inhibitory synapses, within SCN core between both genotypes. However, in the asymmetric, and therefore putative excitatory/glutamatergic synapses, the size of the presynaptic terminal and the distance of the vesicles to the synaptic cleft was larger in Bmal1−/− mice. In contrast to a study on the cerebral cortex in older Bmal1−/− mice with neurodegeneration (Musiek et al., 2013), we did not see a reduction in the number of synaptic vesicles. This discrepancy could be due to the neurodegeneration associated with accelerated aging or to differences in brain regions. Vesicles with a shorter distance to the presynaptic membrane are particularly important for the immediate release of transmitters by the readily releasable pool and thus synaptic strength (Kaeser and Regehr, 2017). The increased distance of the vesicles from the presynaptic membrane in Bmal1−/− mice may, hence, contribute to reduced synaptic efficacy (Kaeser and Regehr, 2017). Thus, our data suggests that the efficacy of the synapse between the ipRGC and the SCN neurons at the structural level is affected by the Bmal1-deletion. Furthermore, there is evidence that Bmal1 rhythmically regulates the synaptic plasticity in the hippocampus by modulating the activity of

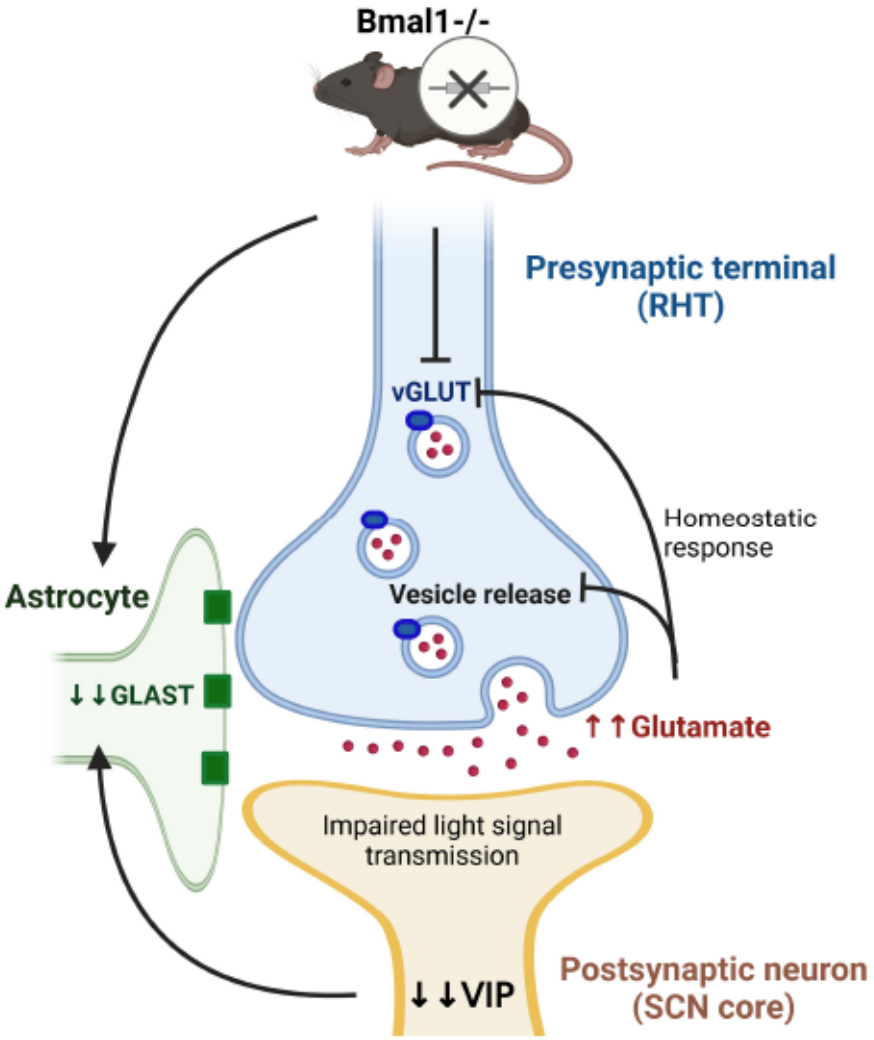

FIGURE 8
Schematic diagram showing that Bmal1-deletion affects the glutamate transmission at the tripartite synapse between the ipRGCs and the VIP-neurons in the SCN (Created in https://BioRender.com).

synaptic calmodulin kinase (CamKII*a*) (Barone et al., 2023), which is involved in maintaining an optimal range of glutamate release probability (Hinds et al., 2003). Almost all SCN neurons are GABAergic (Reghunandanan and Reghunandanan, 2006; Varadarajan et al., 2018; Wen et al., 2020). The glutamate is released in SCN mainly via RHT terminals (in combination with PACAP) in response to light during the day to mediate light-induced neuronal firing and by astrocytes during the night to increase the presynaptic GABA release and consequently suppress the postsynaptic neuronal activity (Brancaccio et al., 2019; Brancaccio

et al., 2017; Reghunandanan and Reghunandanan, 2006). It is debatable that intrinsic glutamatergic neurons in SCN exist. On one hand, it has been shown that glutamate immunoreactivity was occasionally found in non-retinal terminals (de Vries et al., 1993). In addition, some glutamate-immunoreactive nerve cell bodies were identified in the ventral and dorsal SCN of Wistar rats (Hannibal et al., 2000). Also, glutamate was rhythmically released in the organotypic slice cultures of the rat SCN (Shinohara et al., 1998); however, it is not clear if the glutamate is of neuronal or astrocytic origin. On the other hand, using *in situ* hybridization data from the Allen Brain Institute,[2] there was no expression of vGLUT1 and vGLUT2 mRNA (markers of glutamatergic neurons) in SCN.

Importantly, the SCN core receives other input fibers such as geniculo-hypothalamic tract (GHT) (Hundahl et al., 2012) which release contain NPY and GABA (Hundahl et al., 2010; Francois-Bellan et al., 1990). For a precise identification of RHT nerve terminals that target the VIP cells, colocalization of ipRGCs tracer and VIP staining at the synapses in future studies is of crucial significance.

Excitotoxicity is prevented both by a homeostatic autoregulatory mechanism that limits excessive glutamate release by presynaptic vesicles (Winter and Ueda, 2008; Daniels et al., 2004) and by astrocytic glutamate reuptake via GLAST (Todd and Hardingham, 2020). In the SCN of Bmal1-deficient mice, GLAST-Ir was significantly reduced and glutamate levels were significantly increased, indicating an insufficient glutamate reuptake mechanism. Therefore, the reduced vGLUT-Ir in the Bmal1-/- mice could be a consequence of the homeostatic response to excess glutamate. Our data are consistent with a reduction of GLAST and insufficient glutamate reuptake in clock gene-deficient cortical astrocytes (Beaulé et al., 2009). Similarly, in mice with conditional deletion of Bmal1 in GLAST-expressing astrocytes, glutamate levels in the cerebrospinal fluid are significantly increased (Barca-Mayo et al., 2020). These data suggest that the molecular clockwork plays a role in modulating extracellular glutamate availability and thereby also in preventing excitotoxicity in the central nervous system, which is implicated in the pathogenesis of neurodegenerative diseases (Cuellar-Santoyo et al., 2023). Increased excitotoxicity could contribute to progressive neurodegeneration, which is evident in older Bmal1−/− mice and has so far been mainly attributed to increased oxidative stress (Musiek et al., 2013). Interestingly, in the hippocampus, spine size is inversely correlated with the efficacy of local glutamate uptake and thus appears to determine the probability of synaptic crosstalk (Herde et al., 2020). Thus, the enlargement of the presynaptic terminals in the SCN of the Bmal1−/− mice could be related to the lower efficacy of glutamate uptake. Our previous data showed that glial synaptic coverage is reduced in the hippocampal mossy fiber synapses of young Bmal1−/− (Ali et al., 2020). It is, therefore, very likely that Bmal1 deficiency affects the structure-function relationships of the glutamatergic tripartite synapses in large parts of the brain.

In the SCN, VIP-neurons are excited in response to light, leading to release of VIP (Jones et al., 2018; Todd et al., 2020), which is crucial for rhythm robustness (Hamnett et al., 2019). We observed a decrease in VIP-Ir in Bmal1−/− mice, consistent with an impairment in behavioral response to light and rhythm stability and in line with our previous study, which showed that Bmal1 deletion affects the light-induced neuronal activity in SCN during day-time (Öztürk et al., 2021). We assume that this reduction is, at least partially, due to impaired glutamate transmission at the SCN tripartite synapse and hence, altered light input to VIP-neurons, as a consequence of a defect molecular clockwork in the neurons and astrocytes. Consistently, astrocytic Bmal1 deletion affects VIP-Ir (Barca-Mayo et al., 2017). On the other hand, VIP modulates astrocytic GLAST activity (Goursaud et al., 2008), indicating a reciprocal relationship between astrocytes and VIP-neurons in the SCN.

In conclusion, our data suggests that Bmal1-deletion affects the glutamate neurotransmission in the SCN (Figure 8). Further studies are needed to determine the molecular clockwork influence on other photic image-forming and non-image-forming brain functions in a similar manner. This would have far-reaching implications related to the modulation of various brain functions and possibly also increased excitotoxicity through chronodisruption.

Data availability statement

The datasets presented in this study can be found in online repositories. The names of the repository/repositories and accession number(s) can be found below: https://researchdata.hhu.de/handle/entry/180, 2024-12-03T13:41:42Z.

Ethics statement

The animal study was approved by the North Rhine-Westphalia State Agency for Nature, Environment and Consumer Protection (LANUV), Germany (approval number: 84.02.04.2012 A102, 84-02.04.2014. A314). The study was conducted in accordance with the local legislation and institutional requirements.

Author contributions

HK: Data curation, Formal Analysis, Investigation, Methodology, Software, Validation, Visualization, Writing – original draft. MA: Formal Analysis, Methodology, Software, Visualization, Writing – review and editing. TW: Data curation, Formal Analysis, Software, Validation, Visualization, Writing – review and editing. BF: Data curation, Formal Analysis, Investigation, Methodology, Writing – original draft. AH: Methodology, Validation, Writing – review and editing. AB: Methodology, Software, Validation, Visualization, Writing – review and editing. EN: Formal Analysis, Software, Writing – review and editing. FG: Data curation, Methodology, Software, Writing – review and editing. FT-L: Methodology, Validation, Visualization, Writing – review and editing. FP: Formal Analysis, Software, Writing – review and editing. KB: Methodology, Writing – review and editing. LG: Formal Analysis, Methodology, Resources,

2 http://mouse.brain-map.org

Writing – review and editing. DW: Methodology, Resources, Writing – review and editing. CG: Conceptualization, Funding acquisition, Investigation, Project administration, Resources, Supervision, Validation, Visualization, Writing – original draft, Writing – review and editing. AA: Conceptualization, Formal Analysis, Investigation, Methodology, Software, Supervision, Validation, Visualization, Writing – original draft, Writing – review and editing.

Funding

The authors declare that financial support was received for the research, authorship, and/or publication of this article. This study was supported by a grant from the German Research Foundation (DFG) (Grant number: INST 1358/55-1 FUGG). This Publication was supported by Heinrich Heine University, Düsseldorf, Germany (number: ULBD-24-28750).

Acknowledgments

We thank Hanna Bellert, Ursula Lammersen, Ralf Fassbender for excellent technical assistance. We thank Jane K. Schröder and Hussein Haidar for their support in image acquisition.

Conflict of interest

The authors declare that the research was conducted in the absence of any commercial or financial relationships that could be construed as a potential conflict of interest.

Generative AI statement

The authors declare that no Generative AI was used in the creation of this manuscript.

Publisher's note

Supplementary material

The Supplementary Material for this article can be found online at: https://www.frontiersin.org/articles/10.3389/fncel.2025.1538985/full#supplementary-material

References

Ali, A. A. H., Schwarz-Herzke, B., Rollenhagen, A., Anstötz, M., Holub, M., Lübke, J., et al. (2020). Bmal1-deficiency affects glial synaptic coverage of the hippocampal mossy fiber synapse and the actin cytoskeleton in astrocytes. *Glia* 68, 947–962. doi: 10.1002/glia.23754

Ali, A. A., Schwarz-Herzke, B., Stahr, A., Prozorovski, T., Aktas, O., and von Gall, C. (2015). Premature aging of the hippocampal neurogenic niche in adult Bmal1-deficient mice. *Aging (Albany NY)* 7, 435–449. doi: 10.18632/aging.100764

Baba, K., Piano, I., Lyuboslavsky, P., Chrenek, M. A., Sellers, J. T., Zhang, S., et al. (2018). Removal of clock gene Bmal1 from the retina affects retinal development and accelerates cone photoreceptor degeneration during aging. *Proc. Natl. Acad. Sci. U S A.* 115, 13099–13104. doi: 10.1073/pnas.1808137115

Barca-Mayo, O., Boender, A. J., Armirotti, A., and de Pietri Tonelli, D. (2020). Deletion of astrocytic BMAL1 results in metabolic imbalance and shorter lifespan in mice. *Glia* 68, 1131–1147. doi: 10.1002/glia.23764

Barca-Mayo, O., Pons-Espinal, M., Follert, P., Armirotti, A., Berdondini, L., and de Pietri Tonelli, D. (2017). Astrocyte deletion of Bmal1 alters daily locomotor activity and cognitive functions via GABA signalling. *Nat. Commun.* 8:14336. doi: 10.1038/ncomms14336

Barone, I., Gilette, N. M., Hawks-Mayer, H., Handy, J., Zhang, K. J., Chifamba, F. F., et al. (2023). Synaptic BMAL1 phosphorylation controls circadian hippocampal plasticity. *Sci. Adv.* 9:eadj1010. doi: 10.1126/sciadv.adj1010

Beaulé, C., Swanstrom, A., Leone, M. J., and Herzog, E. D. (2009). Circadian modulation of gene expression, but not glutamate uptake, in mouse and rat cortical astrocytes. *PLoS One* 4:e7476. doi: 10.1371/journal.pone.0007476

Beier, C., Zhang, Z., Yurgel, M., and Hattar, S. (2021). Projections of ipRGCs and conventional RGCs to retinorecipient brain nuclei. *J. Comp. Neurol.* 529, 1863–1875. doi: 10.1002/cne.25061

Berson, D. M., Dunn, F. A., and Takao, M. (2002). Phototransduction by retinal ganglion cells that set the circadian clock. *Science* 295, 1070–1073. doi: 10.1126/science.1067262

Boccuni, I., and Fairless, R. (2022). Retinal glutamate neurotransmission: From physiology to pathophysiological mechanisms of retinal ganglion cell degeneration. *Life* 12:638. doi: 10.3390/life12050638

Brancaccio, M., Edwards, M. D., Patton, A. P., Smyllie, N. J., Chesham, J. E., Maywood, E. S., et al. (2019). Cell-autonomous clock of astrocytes drives circadian behavior in mammals. *Science* 363, 187–192. doi: 10.1126/science.aat4104

Brancaccio, M., Patton, A. P., Chesham, J. E., Maywood, E. S., and Hastings, M. H. (2017). Astrocytes control circadian timekeeping in the suprachiasmatic nucleus via glutamatergic signaling. *Neuron* 93, 1420–1435.e5. doi: 10.1016/j.neuron.2017.02.030

Brown, D. R. (2000). Neuronal release of vasoactive intestinal peptide is important to astrocytic protection of neurons from glutamate toxicity. *Mol. Cell. Neurosci.* 15, 465–475. doi: 10.1006/mcne.2000.0840

Bunger, M. K., Wilsbacher, L. D., Moran, S. M., Clendenin, C., Radcliffe, L. A., Hogenesch, J. B., et al. (2000). Mop3 is an essential component of the master circadian pacemaker in mammals. *Cell* 103, 1009–1017. doi: 10.1016/S0092-8674(00)00205-1

Cagampang, F. R., Rattray, M., Powell, J. F., Campbell, I. C., and Coen, C. W. (1996). Circadian changes of glutamate decarboxylase 65 and 67 mRNA in the rat suprachiasmatic nuclei. *Neuroreport* 7, 1925–1928. doi: 10.1097/00001756-199608120-00011

Chi-Castañeda, D., and Ortega, A. (2018). Circadian regulation of glutamate transporters. *Front. Endocrinol.* 9:340. doi: 10.3389/fendo.2018.00340

Colwell, C. S., Michel, S., Itri, J., Rodriguez, W., Tam, J., Lelievre, V., et al. (2004). Selective deficits in the circadian light response in mice lacking PACAP. *Am. J. Physiol. Regul. Integr. Comp. Physiol.* 287, R1194–R1201. doi: 10.1152/ajpregu.00268.2004

Cuellar-Santoyo, A. O., Ruiz-Rodríguez, V. M., Mares-Barbosa, T. B., Patrón-Soberano, A., Howe, A. G., Portales-Pérez, D. P., et al. (2023). Revealing the contribution of astrocytes to glutamatergic neuronal transmission. *Front. Cell. Neurosci.* 16:1037641. doi: 10.3389/fncel.2022.1037641

Daniels, R. W., Collins, C. A., Gelfand, M. V., Dant, J., Brooks, E. S., Krantz, D. E., et al. (2004). Increased expression of the Drosophila vesicular glutamate transporter

leads to excess glutamate release and a compensatory decrease in quantal content. *J. Neurosci.* 24, 10466–10474. doi: 10.1523/JNEUROSCI.3001-04.2004

Darna, M., Schmutz, I., Richter, K., Yelamanchili, S. V., Pendyala, G., Höltje, M., et al. (2009). Time of day-dependent sorting of the vesicular glutamate transporter to the plasma membrane. *J. Biol. Chem.* 284, 4300–4307. doi: 10.1074/jbc.M805480200

de Vries, M. J., Cardozo, B. N., van der Want, J., de Wolf, A., and Meijer, J. H. (1993). Glutamate immunoreactivity in terminals of the retinohypothalamic tract of the brown Norwegian rat. *Brain Res.* 612, 231–237. doi: 10.1016/0006-8993(93)91665-F

Engelund, A., Fahrenkrug, J., Harrison, A., and Hannibal, J. (2010). Vesicular glutamate transporter 2 (VGLUT2) is co-stored with PACAP in projections from the rat melanopsin-containing retinal ganglion cells. *Cell Tissue Res.* 340, 243–255. doi: 10.1007/s00441-010-0950-3

Fernandez, D. C., Fogerson, P. M., Lazzerini Ospri, L., Thomsen, M. B., Layne, R. M., Severin, D., et al. (2018). Light affects mood and learning through distinct retina-brain pathways. *Cell* 175, 71–84.e18. doi: 10.1016/j.cell.2018.08.004

Francois-Bellan, A. M., Kachidian, P., Dusticier, G., Tonon, M. C., Vaudry, H., and Bosler, O. (1990). GABA neurons in the rat suprachiasmatic nucleus: Involvement in chemospecific synaptic circuitry and evidence for GAD-peptide colocalization. *J. Neurocytol.* 19, 937–947. doi: 10.1007/BF01186821

Fremeau, R. T., Kam, K., Qureshi, T., Johnson, J., Copenhagen, D. R., Storm-Mathisen, J., et al. (2004). Vesicular glutamate transporters 1 and 2 target to functionally distinct synaptic release sites. *Science* 304, 1815–1819. doi: 10.1126/science.1097468

Fremeau, R. T., Troyer, M. D., Pahner, I., Nygaard, G. O., Tran, C. H., and Reimer, R. J. (2001). The expression of vesicular glutamate transporters defines two classes of excitatory synapse. *Neuron* 31, 247–260. doi: 10.1016/S0896-6273(01)00344-0

Girardet, C., Blanchard, M. P., Ferracci, G., Lévêque, C., Moreno, M., François-Bellan, A. M., et al. (2010). Daily changes in synaptic innervation of VIP neurons in the rat suprachiasmatic nucleus: Contribution of glutamatergic afferents. *Eur. J. Neurosci.* 31, 359–370. doi: 10.1111/j.1460-9568.2009.07071.x

Gompf, H. S., Fuller, P. M., Hattar, S., Saper, C. B., and Lu, J. (2015). Impaired circadian photosensitivity in mice lacking glutamate transmission from retinal melanopsin cells. *J. Biol. Rhythms* 30, 35–41. doi: 10.1177/0748730414561545

Goursaud, S., Maloteaux, J. M., and Hermans, E. (2008). Activation of VIP/PACAP type 2 receptor by the peptide histidine isoleucine in astrocytes influences GLAST-mediated glutamate uptake. *J. Neurochem.* 105, 1165–1175. doi: 10.1111/j.1471-4159.2008.05231.x

Hamnett, R., Crosby, P., Chesham, J. E., and Hastings, M. H. (2019). Vasoactive intestinal peptide controls the suprachiasmatic circadian clock network via ERK1/2 and DUSP4 signalling. *Nat. Commun.* 10:542. doi: 10.1038/s41467-019-08427-3

Hannibal, J., Moller, M., Ottersen, O. P., and Fahrenkrug, J. (2000). PACAP and glutamate are co-stored in the retinohypothalamic tract. *J. Comp. Neurol.* 418, 147–155. doi: 10.1002/(SICI)1096-9861(20000306)418:2<147::AID-CNE2>3.0.CO;2-#

Hassan, S. A., Ali, A. A. H., Yassine, M., Sohn, D., Pfeffer, M., Jänicke, R. U., et al. (2021). Relationship between locomotor activity rhythm and corticosterone levels during HCC development, progression, and treatment in a mouse model. *J. Pineal Res.* 70:e12724. doi: 10.1111/jpi.12724

Hattar, S., Liao, H. W., Takao, M., Berson, D. M., and Yau, K. W. (2002). Melanopsin-containing retinal ganglion cells: Architecture, projections, and intrinsic photosensitivity. *Science* 295, 1065–1070. doi: 10.1126/science.1069609

Herde, M. K., Bohmbach, K., Domingos, C., Vana, N., Komorowska-Müller, J. A., Passlick, S., et al. (2020). Local efficacy of glutamate uptake decreases with synapse size. *Cell Rep.* 32:108182. doi: 10.1016/j.celrep.2020.108182

Hinds, H. L., Goussakov, I., Nakazawa, K., Tonegawa, S., and Bolshakov, V. Y. (2003). Essential function of alpha-calcium/calmodulin-dependent protein kinase II in neurotransmitter release at a glutamatergic central synapse. *Proc. Natl. Acad. Sci. U S A.* 100, 4275–4280. doi: 10.1073/pnas.0530202100

Hundahl, C. A., Fahrenkrug, J., Hay-Schmidt, A., Georg, B., Faltoft, B., and Hannibal, J. (2012). Circadian behaviour in neuroglobin deficient mice. *PLoS One* 7:e34462. doi: 10.1371/journal.pone.0034462

Hundahl, C. A., Hannibal, J., Fahrenkrug, J., Dewilde, S., and Hay-Schmidt, A. (2010). Neuroglobin expression in the rat suprachiasmatic nucleus: Colocalization, innervation, and response to light. *J. Comp. Neurol.* 518, 1556–1569. doi: 10.1002/cne.22290

Johnson, J., Fremeau, R. T., Duncan, J. L., Rentería, R. C., Yang, H., Hua, Z., et al. (2007). Vesicular glutamate transporter 1 is required for photoreceptor synaptic signaling but not for intrinsic visual functions. *J. Neurosci.* 27, 7245–7255. doi: 10.1523/JNEUROSCI.0815-07.2007

Jones, J. R., Simon, T., Lones, L., and Herzog, E. D. (2018). SCN VIP neurons are essential for normal light-mediated resetting of the circadian system. *J. Neurosci.* 38, 7986–7995. doi: 10.1523/JNEUROSCI.1322-18.2018

Kaeser, P. S., and Regehr, W. G. (2017). The readily releasable pool of synaptic vesicles. *Curr. Opin. Neurobiol.* 43, 63–70. doi: 10.1016/j.conb.2016.12.012

Kim, K. Y., Rios, L. C., Le, H., Perez, A. J., Phan, S., Bushong, E. A., et al. (2019). Synaptic specializations of melanopsin-retinal ganglion cells in multiple brain regions revealed by genetic label for light and electron microscopy. *Cell Rep.* 29, 628–644.e6. doi: 10.1016/j.celrep.2019.09.006

Kiss, J., Halász, B., Csáki, A., Liposits, Z., and Hrabovszky, E. (2007). Vesicular glutamate transporter 2 protein and mRNA containing neurons in the hypothalamic suprachiasmatic nucleus of the rat. *Brain Res. Bull.* 74, 397–405. doi: 10.1016/j.brainresbull.2007.07.023

Koch, K., Hartmann, R., Schröter, F., Suwala, A. K., Maciaczyk, D., Krüger, A. C., et al. (2016). Reciprocal regulation of the cholinic phenotype and epithelial-mesenchymal transition in glioblastoma cells. *Oncotarget* 7, 73414–73431. doi: 10.18632/oncotarget.12337

Kondratov, R. V., Kondratova, A. A., Gorbacheva, V. Y., Vykhovanets, O. V., and Antoch, M. P. (2006). Early aging and age-related pathologies in mice deficient in BMAL1, the core componentof the circadian clock. *Genes Dev.* 20, 1868–1873. doi: 10.1101/gad.1432206

Land, P. W., Kyonka, E., and Shamalla-Hannah, L. (2004). Vesicular glutamate transporters in the lateral geniculate nucleus: Expression of VGLUT2 by retinal terminals. *Brain Res.* 996, 251–254. doi: 10.1016/j.brainres.2003.10.032

Lazzerini Ospri, L., Zhan, J. J., Thomsen, M. B., Wang, H., Komal, R., Tang, Q., et al. (2024). Light affects the prefrontal cortex via intrinsically photosensitive retinal ganglion cells. *Sci. Adv.* 10:eadh9251. doi: 10.1126/sciadv.adh9251

LeGates, T. A., Fernandez, D. C., and Hattar, S. (2014). Light as a central modulator of circadian rhythms, sleep and affect. *Nat. Rev. Neurosci.* 15, 443–454. doi: 10.1038/nrn3743

Leone, M. J., Beaule, C., Marpegan, L., Simon, T., Herzog, E. D., and Golombek, D. A. (2015). Glial and light-dependent glutamate metabolism in the suprachiasmatic nuclei. *Chronobiol. Int.* 32, 573–578. doi: 10.3109/07420528.2015.1006328

Mahoney, H. L., and Schmidt, T. M. (2024). The cognitive impact of light: Illuminating ipRGC circuit mechanisms. *Nat. Rev. Neurosci.* 25, 159–175. doi: 10.1038/s41583-023-00788-5

Merchán-Pérez, A., Rodriguez, J. R., Alonso-Nanclares, L., Schertel, A., and Defelipe, J. (2009). Counting synapses using FIB/SEM microscopy: A true revolution for ultrastructural volume reconstruction. *Front. Neuroanat.* 3:18. doi: 10.3389/neuro.05.018.2009

Mrosovsky, N. (1999). Masking: History, definitions, and measurement. *Chronobiol. Int.* 16, 415–429. doi: 10.3109/07420529908998717

Mrosovsky, N., and Hattar, S. (2003). Impaired masking responses to light in melanopsin-knockout mice. *Chronobiol. Int.* 20, 989–999. doi: 10.1081/CBI-120026043

Musiek, E. S., and Holtzman, D. M. (2016). Mechanisms linking circadian clocks, sleep, and neurodegeneration. *Science* 354, 1004–1008. doi: 10.1126/science.aah4968

Musiek, E. S., Lim, M. M., Yang, G., Bauer, A. Q., Qi, L., Lee, Y., et al. (2013). Circadian clock proteins regulate neuronal redox homeostasis and neurodegeneration. *J. Clin. Invest.* 123, 5389–5400. doi: 10.1172/JCI70317

Öztürk, M., Ingenwerth, M., Sager, M., Von Gall, C., and Ali, A. A. H. (2021). Does a red house affect rhythms in mice with a corrupted circadian system? *Int. J. Mol. Sci.* 22:2288. doi: 10.3390/ijms22052288

Panda, S., Provencio, I., Tu, D. C., Pires, S. S., Rollag, M. D., Castrucci, A. M., et al. (2003). Melanopsin is required for non-image-forming photic responses in blind mice. *Science* 301, 525–527. doi: 10.1126/science.1086179

Panda, S., Sato, T. K., Castrucci, A. M., Rollag, M. D., Degrip, W. J., Hogenesch, J. B., et al. (2002). Melanopsin (Opn4) requirement for normal light-induced circadian phase shifting. *Science* 298, 2213–2216. doi: 10.1126/science.1076848

Paxinos, G., and Franklin, K. B. J. (2012). *Paxinos and Franklin's the Mouse Brain in Stereotaxic Coordinates*. Amsterdam: Elsevier.

Pfeffer, M., Korf, H. W., and von Gall, C. (2015). Chronotype and stability of spontaneous locomotor activity rhythm in BMAL1-deficient mice. *Chronobiol. Int.* 32, 81–91. doi: 10.3109/07420528.2014.956218

Pfeffer, M., Müller, C. M., Mordel, J., Meissl, H., Ansari, N., Deller, T., et al. (2009). The mammalian molecular clockwork controls rhythmic expression of its own input pathway components. *J. Neurosci.* 29, 6114–6123. doi: 10.1523/JNEUROSCI.0275-09.2009

Portaluppi, F., Smolensky, M. H., and Touitou, Y. (2010). Ethics and methods for biological rhythm research on animals and human beings. *Chronobiol. Int.* 27, 1911–1929. doi: 10.3109/07420528.2010.516381

Purrier, N., Engeland, W. C., and Kofuji, P. (2014). Mice deficient of glutamatergic signaling from intrinsically photosensitive retinal ganglion cells exhibit abnormal circadian photoentrainment. *PLoS One* 9:e111449. doi: 10.1371/journal.pone.0111449

Reghunandanan, V., and Reghunandanan, R. (2006). Neurotransmitters of the suprachiasmatic nuclei. *J. Circadian Rhythms* 4:2. doi: 10.1186/1740-3391-4-2

Reppert, S. M., and Weaver, D. R. (2002). Coordination of circadian timing in mammals. *Nature* 418, 935–941. doi: 10.1038/nature00965

Romaus-Sanjurjo, D., Custodia, A., Aramburu-Núñez, M., Posado-Fernández, A., Vázquez-Vázquez, L., Camino-Castiñeiras, J., et al. (2021). Symmetric and asymmetric

synapses driving neurodegenerative disorders. *Symmetry* 13:2333. doi: 10.3390/sym13122333

Ruby, N. F., Brennan, T. J., Xie, X., Cao, V., Franken, P., Heller, H. C., et al. (2002). Role of melanopsin in circadian responses to light. *Science* 298, 2211–2213. doi: 10.1126/science.1076701

Shinohara, K., Honma, S., Katsuno, Y., Abe, H., and Honma, K.-I. (1998). Circadian release of amino acids in the suprachiasmatic nucleus in vitro. *NeuroReport* 9, 137–140. doi: 10.1097/00001756-199801050-00027

Spanagel, R., Pendyala, G., Abarca, C., Zghoul, T., Sanchis-Segura, C., Magnone, M. C., et al. (2005). The clock gene Per2 influences the glutamatergic system and modulates alcohol consumption. *Nat. Med.* 11, 35–42. doi: 10.1038/nm1163

Storch, K. F., Paz, C., Signorovitch, J., Raviola, E., Pawlyk, B., Li, T., et al. (2007). Intrinsic circadian clock of the mammalian retina: Importance for retinal processing of visual information. *Cell* 130, 730–741. doi: 10.1016/j.cell.2007.06.045

Todd, A. C., and Hardingham, G. E. (2020). The regulation of astrocytic glutamate transporters in health and neurodegenerative diseases. *Int. J. Mol. Sci.* 21:9607. doi: 10.3390/ijms21249607

Todd, W. D., Venner, A., Anaclet, C., Broadhurst, R. Y., de Luca, R., Bandaru, S. S., et al. (2020). Suprachiasmatic VIP neurons are required for normal circadian rhythmicity and comprised of molecularly distinct subpopulations. *Nat. Commun.* 11:4410. doi: 10.1038/s41467-020-17197-2

Varadarajan, S., Tajiri, M., Jain, R., Holt, R., Ahmed, Q., Lesauter, J., et al. (2018). Connectome of the suprachiasmatic nucleus: New evidence of the core-shell relationship. *eNeuro* 5:e0205-18.20181–14. doi: 10.1523/ENEURO.0205-18.2018

von Gall, C. (2022). The effects of light and the circadian system on rhythmic brain function. *Int. J. Mol. Sci.* 23:2778. doi: 10.3390/ijms23052778

Wen, S. A., Ma, D., Zhao, M., Xie, L., Wu, Q., Gou, L., et al. (2020). Spatiotemporal single-cell analysis of gene expression in the mouse suprachiasmatic nucleus. *Nat. Neurosci.* 23, 456–467. doi: 10.1038/s41593-020-0586-x

Winter, H. C., and Ueda, T. (2008). The glutamate uptake system in presynaptic vesicles: Further characterization of structural requirements for inhibitors and substrates. *Neurochem. Res.* 33, 223–231. doi: 10.1007/s11064-007-9493-8

Wojcik, S. M., Rhee, J. S., Herzog, E., Sigler, A., Jahn, R., Takamori, S., et al. (2004). An essential role for vesicular glutamate transporter 1 (VGLUT1) in postnatal development and control of quantal size. *Proc. Natl. Acad. Sci. U S A.* 101, 7158–7163. doi: 10.1073/pnas.0401764101

Yang, G., Chen, L., Zhang, J., Ren, B., and Fitzgerald, G. A. (2019). Bmal1 deletion in mice facilitates adaptation to disrupted light/dark conditions. *JCI Insight* 5:e125133. doi: 10.1172/jci.insight.125133

Yelamanchili, S. V., Pendyala, G., Brunk, I., Darna, M., Albrecht, U., and Ahnert-Hilger, G. (2006). Differential sorting of the vesicular glutamate transporter 1 into a defined vesicular pool is regulated by light signaling involving the clock gene Period2. *J. Biol. Chem.* 281, 15671–15679. doi: 10.1074/jbc.M600378200

Zhang, Z., Beier, C., Weil, T., and Hattar, S. (2021). The retinal ipRGC-preoptic circuit mediates the acute effect of light on sleep. *Nat. Commun.* 12:5115. doi: 10.1038/s41467-021-25378-w

4. Discussion

Bmal1 is an essential component of the molecular clockwork in neurons and glia. Conventional knockout of Bmal1 (Bunger et al., 2000) as well as conditional deletion in forebrain neurons (Izumo et al., 2014) leads to loss of rhythmic locomotor activity under constant conditions. In addition, astrocytic-specific Bmal1 deletion results in shortened active periods and bimodal behavior (Barca-Mayo et al., 2017). Although the circadian rhythmicity is lost in Bmal1-/- mice, previous studies (Bunger et al., 2000, Pfeffer et al., 2015, Yang et al., 2019) showed that the negative masking response to light was intact. In agreement with these reports, Bmal1-/- mice displayed less locomotor activity during the light phase than the dark phase, suggesting that the inhibitory effect of light on the locomotor activity is still present. However, the activity percentage during the light phase was higher than in the control mice, indicating that the masking response to light in Bmal1-/- is less than in the controls. This is reminiscent of a previous study, which showed that a 1-hour light pulse at night reduced the wheel running activity of Clock mutant mice less than wild type, suggesting a decreased light sensitivity leading to reduced negative masking (Redlin et al., 2005). Besides, in Bmal1-/- mice, the light-induced per1 and per2 expression was decreased, probably due to dysfunctional light-induced ryanodine-calcium signaling in SCN (Pfeffer et al., 2009). These data suggest that the circadian clock component Bmal1 may play a dual role as a molecular oscillator and regulator of light perception and, in turn, mediating the inhibitory effect of light on locomotor activity. The amplitude of the activity rhythm was significantly dampened in Bmal1-deficient mice in line with decreased stability of rhythmic locomotor activity and later chronotype in Bmal1-/- mice (Pfeffer et al., 2015). Nevertheless, the total activity count was not altered in contrast to previously reported reduced total spontaneous locomotor activity (Pfeffer et al., 2015) and wheel running in Bmal1-/- mice (Bunger et al., 2000). Taken all together, we assume that Bmal1 deletion decreases the stability of locomotor activity under standard photoperiod and reduces the negative masking response to light.

The reduction in negative masking response to light may be attributable to decreased sensitivity of the circadian system to light (Redlin et al., 2005). Previous observations did not show gross morphological changes in the retina of global or glial-specific Bmal1-deficient mice (Riccitelli et al., 2022, Storch et al., 2007). Though specific Bmal1 deletion in the retina results in an age-dependent thinning of the retinal layer and accelerated

impairment of cone cell structure and function as well as stunted dendritic processes of rod bipolar cells in the OPL (Baba et al., 2018). Our morphological analysis of the retinal layer was in agreement with these observations and showed the presence of all retinal layers and a reduction in the thickness of the IPL as well as the rods and cones layer, which may indicate slight retinal degeneration in Bmal1-/- mice.

Both rods/cones photoreceptors and melanopsin-expressing ipRGCs contribute to negative masking. However, the rod/cone system may be responsible for positive masking as well, because it depends on the form of vision and is strongly attenuated in mice with retinal degeneration (Mrosovsky et al., 2000). Thus, the decreased locomotor activity during the dark phase in Bmal1-/- may be interpreted as reduced positive masking due to degeneration of the rod and cone layer. The number of melanopsin-immunoreactive ipRGCs was comparable in Bmal1-/-, and perhaps, this preserved some degree of negative masking response to light, in line with observations in Clock mutant mice (Redlin et al., 2005). This also indicates that the behavioral changes in Bmal1-/- mice are less likely due to impairment of light-sensitive photopigment melanopsin.

Previous studies indicated that Bmal1 deficiency altered the retinal neuronal activity in response to light (Riccitelli et al., 2022, Storch et al., 2007). Importantly, neuronal activity is critically influenced by neurotransmission (Teleanu et al., 2022). Specifically, glutamate is the predominant neurotransmitter in the retina. Thus, alteration of glutamatergic signaling could greatly influence the neuronal activity within the retina. Glutamatergic signaling essentially relies on glutamate sequestration into the synaptic vesicles via the vesicular glutamate transporters (Engelund et al., 2010). VGLUT1 and VGLUT2 are the main vesicular glutamate transporters in the central nervous system that are expressed in a non-overlapping complementary fashion, suggesting a different functional role (Fremeau et al., 2001).

In the retina, the VGLUT1 is expressed mainly in the two retinal synaptic layers, OPL and IPL, and is involved in rods and cones-driven image-forming signaling (Johnson et al., 2007), while VGLUT2 is expressed predominantly in the RGC and mediates the non-image-forming visual response in the brain (Land et al., 2004). Interestingly, VGLUT1 immunoreaction levels were upregulated in the OPL of Bmal1-/- mice. This may be a compensatory upregulation due to morphological changes in the photoreceptor layer. In contrast, the expression of VGLUT2 in the RGCs was decreased in Bmal1-deficient mice, indicating altered glutamatergic transmission within the retina of Bmal1-deficient mice. The previous report showed that VGLUT2, in particular, plays an essential role in light-

induced circadian functions, as mice with selective VGLUT2 deletion in ipRGC show impaired non-image-forming functions, including entrainment, masking response, and pupillary light reflex, as well as failure of c-Fos induction in the SCN following a light pulse (Gompf et al., 2015, Purrier et al., 2014), while these functions were preserved in VGLUT1 knockout mice (Johnson et al., 2007). Hence, the defective negative masking in Bmal11-/- is likely related to altered glutamatergic transmission in RGCs via reduced VGLUT2.

Light information is then transmitted by axons of ipRGCs to the master clock in SCN via glutamate release, which induces the responses to light at both the cellular and the behavioral levels (Vindlacheruvu et al., 1992).

Thus, we investigated the vesicular glutamate transporter in the SCN. Both VGLUT1 and VGLUT2 were expressed in SCN, with higher expression levels of VGLUT2, in agreement with previous observations showing that VGLUT2 is the main vesicular transporter used by the ipRGCs to mediate the light signal transmission to SCN (Engelund et al., 2010). The number of VGLUT1 and VGLUT2-immunoreactive particles was less in the SCN of Bmal1-/- mice, in agreement with previous studies indicating that glutamate transporters are regulated by the circadian clock. For instance, VGLUT1 protein oscillates under a normal light/dark cycle as well as under constant darkness, while this oscillation was absent in per2-mutant mice (Yelamanchili et al., 2006). Similarly, VGLUT2 mRNA and protein levels show rhythmic changes in the rat SCN (Kiss et al., 2007). In addition, the dynamics of the vesicular glutamate transporters display time-of-day-dependent alterations (Darna et al., 2009). Furthermore, the density of VGLUT1- and VGLUT2-labeled terminals, specifically, on VIP-expressing neurons increased during the day in rat SCN, suggesting a selective synaptic remodeling at sites of photic integration (Girardet et al., 2010). Therefore, the decreased number of VGLUT2-immunoreactive particles in the ventral SCN, the principal retinal input region, may be correlated to the defective masking in Bmal1-/-. This is also consistent with a previous study using mouse models with impaired masking that showed decreased expression of VGLUT2 in SCN (Pfeffer et al., 2018). Importantly, VGLUT1 and VGLUT2 levels significantly decreased with age in rats (Ménard et al., 2015), which is also in line with the premature aging phenotype reported in Bmal1-ko mice (Kondratov et al., 2006).

Noteworthy, it is still controversial if the SCN is the core regulator of masking (Gall and Shuboni-Mulligan, 2022). Here, we assume that a change in light input to SCN may affect the sensitivity of the circadian system to light and the fine-tuning of light information,

since the negative masking response to light was reduced in Bmal1-/-, although still intact.

Astrocytes have been shown to be an important contributor to the circadian timekeeping in SCN via intercellular communications with the neurons and by modulating glutamatergic signaling (Barca-Mayo et al., 2017). The astrocytes regulate the extracellular glutamate level by both glutamate release and precise glutamate reuptake, which is mediated mainly via GLAST and GLT-1, by the fine astrocytic processes surrounding the synaptic cleft to avoid neuronal excitotoxicity (Brancaccio et al., 2019, Chi-Castañeda and Ortega, 2018). Diurnal fluctuation in astrocytic glutamate reuptake and glutamine synthetase activity has been reported (Leone et al., 2015).

Importantly, GLAST seems to be regulated by the astrocytic molecular clock (Beaulé et al., 2009) and shows diurnal variations in its mRNA and protein levels in SCN (Cagampang et al., 1996). In Per2 mutant mice, a decreased GLAST level and an increased extracellular glutamate level as well as decreased glutamate reuptake by cultured Per2-deficient astrocytes have been reported (Spanagel et al., 2005). A similar observation was reported in Clock-, Per2-, or NPAS2-deficient cortical astrocytes as the GLAST mRNA and protein levels were significantly reduced, leading to decreased glutamate reuptake (Beaulé et al., 2009). However, this seems to be region-specific, as the relative expression of GLAST and GLT-1 on the plasma membrane in the hippocampus did not show diurnal change (McCauley et al., 2020). We showed earlier that Bmal1 deficiency was associated with altered decreased glial coverage of the hippocampal tripartite synapses (Ali et al., 2020). This retraction of the fine astrocytic processes may be correlated with a decreased astrocytic reuptake ability and improper neurotransmitter signaling. In line with this notion, Barca-Mayo reported that Bmal1 deletion leads to decreased astrocytic GABA reuptake and increased GABA levels in CSF and the hypothalamus, which may contribute to altered circadian locomotor behavior as well as cognitive deficits (Barca-Mayo et al., 2020, Barca-Mayo et al., 2017). Likewise, Bmal1 deficiency resulted in upregulated glutamate levels in CSF (Barca-Mayo et al., 2020). These data are in agreement with our findings, as the glutamate level in SCN was higher in Bmal1-deficient mice. Indeed, a decreased glutamate reuptake capacity and a reduction of high-affinity glutamate transporters have been reported in glutamatergic terminals of aged rats (Segovia et al., 2001), which is also in line with the premature aging phenotype observed in Bmal1-deficient mice (Kondratov et al., 2006). Importantly, negative feedback of glutamate analogues on the VGLUT activity (Winter and Ueda,

2008). This suggests that the increased glutamate levels may contribute to the here-observed decrease of VGLUT-Ir in Bmal1-/-. In sum, our findings support that Bmal1 deficiency may lead to decreased glutamate reuptake by astrocytes and upregulated glutamate levels in SCN.

The circadian cycle could also modulate the synaptic transmission via inducing morphological alteration; for instance, the sleep-wake cycle regulates synaptic homeostasis (Cirelli and Tononi, 2020). Interestingly, ultrastructure studies showed that Bmal1 localizes in the hippocampal synapses and regulates the circadian rhythms of CaMKIIα-phosphorylation and hence locally gates the circadian rhythmicity of synaptic plasticity (Barone et al., 2023).

To get deeper insights into the effect of Bmal1 deletion on the structural integrity of the synapses, we performed ultrastructural analysis of SCN core region synapses. Here, we didn't notice an obvious difference in the overall morphology of the synapses consistent with previous observations in the retinal synapses (Storch et al., 2007). However, this contrasts with the synaptic degeneration observed in the retrosplenial cortex in 6-month-old Bmal1-deficient mice (Musiek et al., 2013). Musiek and colleagues reported that Bmal1 KO mice showed both normal and abnormal terminals where the synaptic terminals are swollen and relatively devoid of synaptic vesicles (Musiek et al., 2013). In line with this observation, we report that the presynaptic terminals of excitatory asymmetric synapses in Bmal1-deficient mice were larger than the wild type; however, the number of synaptic vesicles seemed indistinguishable. This discrepancy could rely on the age difference between mice used in the studies, as the aging effect of Bmal1 deletion starts around 4 months and becomes tremendously progressive with age (Kondratov et al., 2006, Kondratova et al., 2010). Interestingly, a recent study reported that the efficacy of glutamate reuptake negatively correlates with the size of synapses due to a decreased relative synaptic coverage by astrocytic fine processes (Herde et al., 2020). Our previous data showed that Bmal1 deficiency reduces glial synaptic coverage of the hippocampal mossy fiber synapses (Ali et al., 2020). This may rely on the increased size of the presynaptic terminal and may contribute to the higher glutamate levels in SCN tissue observed in this study.

Importantly, only a small fraction of vesicles in the presynaptic bouton are available for immediate release and thus form the readily releasable pool (RRP). The RRP can also be tentatively identified as docked synaptic vesicles (Rosenmund and Stevens, 1996), and nearby undocked vesicles (proximal pole) that could be rapidly recruited to unoccupied

activated sites on the presynaptic membrane to contribute to the RRP (Gundelfinger et al., 2003, Kaeser and Regehr, 2017). Thus, the RRP availability could be correlated to the distance between the vesicle and the presynaptic membrane. In Bmal1-/- mice, the distance between the vesicles and the presynaptic membrane was increased, which may reflect a reduced RRP in the excitatory synapses and could lead to a decreased synaptic strength (Kaeser and Regehr, 2017). Thus, the absence of Bmal1 may affect the vesicle dynamics in the presynaptic terminals, in agreement with a previous study (Barone et al., 2023). The elevated glutamate levels may also play a role in these morphological alterations, as excess glutamate may induce a compensatory decrease in presynaptic vesicle release to avoid exaggerated synaptic excitation (Daniels et al., 2004). Importantly, the presynaptic terminals of symmetric synapses were morphologically indistinguishable between both genotypes, which indicates that this effect was limited to the excitatory synapses in Bmal1-deficient mice.

The glutamatergic terminals of the retinohypothalamic tract innervate mainly the VIP-containing neurons in the core region of the SCN (Kim et al., 2019). SCN VIP neurons are excited in response to light, leading to the release of VIP (Jones et al., 2018, Todd and Hardingham, 2020), which represents a potent synchronizer for the SCN and is capable of reprogramming the circadian rhythmicity at the cellular and network level to obtain a robust coherent firing rhythm (Hamnett et al., 2019). VIP is also crucial for the neuron-astrocyte interaction and enhances the glutamate reuptake by the astrocytes (Brown, 2000) by a GLAST-mediated mechanism (Goursaud et al., 2008).

Importantly, the influence of VIP on the circadian system seems to be bidirectional and not only dependent on light, as circadian rhythms of VIP release in rat SCN slices (Shinohara et al., 1994) and VIP mRNA in the mouse SCN (Dardente et al., 2004) were observed under constant conditions. Moreover, the diurnal oscillation of VIP immunoreaction in mouse SCN was lost upon astrocytic Bmal1 deletion (Barca-Mayo et al., 2017) indicating that VIP is regulated by the molecular clock components. Here, we report a decreased VIP immunoreaction in the SCN of Bmal1-deficient mice. This reduction could be due to impaired light input to SCN neurons via altered glutamatergic transmission in Bmal1-knockout mice. Although Barca-Mayo et al. reported on astrocytic-specific Bmal1 deletion, there was an increase in the neuronal VIP intensity in the SCN at ZT12. It is noteworthy that in our mouse model Bmal1 is globally deficient, also in SCN neurons, which could induce an additional intra-neuronal effect leading to a decreased VIP. We assume that the impaired VIP in Bmal1-deficient mice may result in

a reduced light signal transmission and synchronization among SCN neurons and the integration of light information, leading to aberrant circadian functions, including light-mediated behavior.

In conclusion, the deletion of Bmal1 affects the glutamate transporters and reuptake and induces morphological changes at the excitatory presynaptic terminals within the SCN. The disruptions in the glutamate signaling may impair the light input to the SCN and affect the behavioral responses to light. Importantly, disruption of glutamatergic transmission is involved in multiple neurodegenerative diseases and psychological disorders correlated with chronodisruption. Thus, targeting the molecular clock, including Bmal1, may provide a novel therapeutic strategy to prevent or treat such neurological diseases.

References

ALI, A. A., SCHWARZ-HERZKE, B., STAHR, A., PROZOROVSKI, T., AKTAS, O. & VON GALL, C. 2015. Premature aging of the hippocampal neurogenic niche in adult Bmal1-deficient mice. *Aging (Albany NY),* 7**,** 435-49.

ALI, A. A. H., SCHWARZ-HERZKE, B., ROLLENHAGEN, A., ANSTÖTZ, M., HOLUB, M., LÜBKE, J., ROSE, C. R., SCHNITTLER, H. J. & VON GALL, C. 2020. Bmal1-deficiency affects glial synaptic coverage of the hippocampal mossy fiber synapse and the actin cytoskeleton in astrocytes. *Glia,* 68**,** 947-962.

ALI, A. A. H. & VON GALL, C. 2022. Adult Neurogenesis under Control of the Circadian System. *Cells,* 11.

ASCHOFF, J. 1960. Exogenous and endogenous components in circadian rhythms. *Cold Spring Harb Symp Quant Biol,* 25**,** 11-28.

ATON, S. J., COLWELL, C. S., HARMAR, A. J., WASCHEK, J. & HERZOG, E. D. 2005. Vasoactive intestinal polypeptide mediates circadian rhythmicity and synchrony in mammalian clock neurons. *Nat Neurosci,* 8**,** 476-83.

BABA, K., PIANO, I., LYUBOSLAVSKY, P., CHRENEK, M. A., SELLERS, J. T., ZHANG, S., GARGINI, C., HE, L., TOSINI, G. & IUVONE, P. M. 2018. Removal of clock gene Bmal1 from the retina affects retinal development and accelerates cone photoreceptor degeneration during aging. *Proc Natl Acad Sci U S A,* 115**,** 13099-13104.

BARCA-MAYO, O., BOENDER, A. J., ARMIROTTI, A. & DE PIETRI TONELLI, D. 2020. Deletion of astrocytic BMAL1 results in metabolic imbalance and shorter lifespan in mice. *Glia,* 68**,** 1131-1147.

BARCA-MAYO, O., PONS-ESPINAL, M., FOLLERT, P., ARMIROTTI, A., BERDONDINI, L. & DE PIETRI TONELLI, D. 2017. Astrocyte deletion of Bmal1 alters daily locomotor activity and cognitive functions via GABA signalling. *Nat Commun,* 8**,** 14336.

BARONE, I., GILETTE, N. M., HAWKS-MAYER, H., HANDY, J., ZHANG, K. J., CHIFAMBA, F. F., MOSTAFA, E., JOHNSON-VENKATESH, E. M., SUN, Y., GIBSON, J. M., ROTENBERG, A., UMEMORI, H., TSAI, P. T. & LIPTON, J. O. 2023. Synaptic BMAL1 phosphorylation controls circadian hippocampal plasticity. *Science Advances,* 9**,** eadj1010.

BEAULÉ, C., SWANSTROM, A., LEONE, M. J. & HERZOG, E. D. 2009. Circadian modulation of gene expression, but not glutamate uptake, in mouse and rat cortical astrocytes. *PLoS One,* 4**,** e7476.

BERSON, D. M., CASTRUCCI, A. M. & PROVENCIO, I. 2010. Morphology and mosaics of melanopsin-expressing retinal ganglion cell types in mice. *J Comp Neurol,* 518**,** 2405-22.

BIELLO, S. M., GOLOMBEK, D. A. & HARRINGTON, M. E. 1997. Neuropeptide Y and glutamate block each other's phase shifts in the suprachiasmatic nucleus in vitro. *Neuroscience,* 77**,** 1049-57.

BOUCHARD-CANNON, P., MENDOZA-VIVEROS, L., YUEN, A., KÆRN, M. & CHENG, H. Y. 2013. The circadian molecular clock regulates adult hippocampal neurogenesis by controlling the timing of cell-cycle entry and exit. *Cell Rep,* 5**,** 961-73.

BRANCACCIO, M., EDWARDS, M. D., PATTON, A. P., SMYLLIE, N. J., CHESHAM, J. E., MAYWOOD, E. S. & HASTINGS, M. H. 2019. Cell-autonomous clock of astrocytes drives circadian behavior in mammals. *Science,* 363**,** 187-192.

BROWN, D. R. 2000. Neuronal Release of Vasoactive Intestinal Peptide Is Important to Astrocytic Protection of Neurons from Glutamate Toxicity. *Molecular and Cellular Neuroscience,* 15**,** 465-475.

BUIJS, R. M., VAN EDEN, C. G., GONCHARUK, V. D. & KALSBEEK, A. 2003. The biological clock tunes the organs of the body: timing by hormones and the autonomic nervous system. *J Endocrinol,* 177**,** 17-26.

BUNGER, M. K., WILSBACHER, L. D., MORAN, S. M., CLENDENIN, C., RADCLIFFE, L. A., HOGENESCH, J. B., SIMON, M. C., TAKAHASHI, J. S. & BRADFIELD, C. A. 2000. Mop3 is an essential component of the master circadian pacemaker in mammals. *Cell,* 103**,** 1009-17.

CAGAMPANG, F. R., RATTRAY, M., POWELL, J. F., CAMPBELL, I. C. & COEN, C. W. 1996. Circadian changes of glutamate decarboxylase 65 and 67 mRNA in the rat suprachiasmatic nuclei. *Neuroreport,* 7**,** 1925-8.

CASTEL, M., BELENKY, M., COHEN, S., OTTERSEN, O. P. & STORM-MATHISEN, J. 1993. Glutamate-like immunoreactivity in retinal terminals of the mouse suprachiasmatic nucleus. *Eur J Neurosci,* 5**,** 368-81.

CHEN, D., BUCHANAN, G. F., DING, J. M., HANNIBAL, J. & GILLETTE, M. U. 1999. Pituitary adenylyl cyclase-activating peptide: a pivotal modulator of glutamatergic regulation of the suprachiasmatic circadian clock. *Proc Natl Acad Sci U S A,* 96**,** 13468-73.

CHI-CASTAÑEDA, D. & ORTEGA, A. 2018. Circadian Regulation of Glutamate Transporters. *Front Endocrinol (Lausanne),* 9**,** 340.

CIRELLI, C. & TONONI, G. 2020. Effects of sleep and waking on the synaptic ultrastructure. *Philosophical Transactions of the Royal Society B: Biological Sciences,* 375**,** 20190235.

COLWELL, C. S. 2021. Defining circadian disruption in neurodegenerative disorders. *J Clin Invest,* 131.

DANIELS, R. W., COLLINS, C. A., GELFAND, M. V., DANT, J., BROOKS, E. S., KRANTZ, D. E. & DIANTONIO, A. 2004. Increased expression of the Drosophila vesicular glutamate transporter leads to excess glutamate release and a compensatory decrease in quantal content. *J Neurosci,* 24**,** 10466-74.

DARDENTE, H., MENET, J. S., CHALLET, E., TOURNIER, B. B., PÉVET, P. & MASSON-PÉVET, M. 2004. Daily and circadian expression of neuropeptides in the suprachiasmatic nuclei of nocturnal and diurnal rodents. *Molecular Brain Research,* 124**,** 143-151.

DARNA, M., SCHMUTZ, I., RICHTER, K., YELAMANCHILI, S. V., PENDYALA, G., HÖLTJE, M., ALBRECHT, U. & AHNERT-HILGER, G. 2009. Time of day-dependent sorting of the vesicular glutamate transporter to the plasma membrane. *J Biol Chem,* 284**,** 4300-7.

DHANDE, O. S. & HUBERMAN, A. D. 2014. Retinal ganglion cell maps in the brain: implications for visual processing. *Curr Opin Neurobiol,* 24**,** 133-42.

DICKSON, L. & FINLAYSON, K. 2009. VPAC and PAC receptors: From ligands to function. *Pharmacol Ther,* 121**,** 294-316.

DZIEMA, H. & OBRIETAN, K. 2002. PACAP Potentiates L-Type Calcium Channel Conductance in Suprachiasmatic Nucleus Neurons by Activating the MAPK Pathway. *Journal of Neurophysiology,* 88**,** 1374-1386.

ECKER, J. L., DUMITRESCU, O. N., WONG, K. Y., ALAM, N. M., CHEN, S. K., LEGATES, T., RENNA, J. M., PRUSKY, G. T., BERSON, D. M. & HATTAR, S. 2010. Melanopsin-expressing retinal ganglion-cell photoreceptors: cellular diversity and role in pattern vision. *Neuron,* 67**,** 49-60.

ENGELUND, A., FAHRENKRUG, J., HARRISON, A. & HANNIBAL, J. 2010. Vesicular glutamate transporter 2 (VGLUT2) is co-stored with PACAP in projections from the rat melanopsin-containing retinal ganglion cells. *Cell Tissue Res,* 340**,** 243-55.

ERREN, T. C. & REITER, R. J. 2009. Defining chronodisruption. *Journal of Pineal Research,* 46**,** 245-247.

FARHY-TSELNICKER, I. & ALLEN, N. J. 2018. Astrocytes, neurons, synapses: a tripartite view on cortical circuit development. *Neural Dev,* 13**,** 7.

FERNANDEZ, D. C., CHANG, Y. T., HATTAR, S. & CHEN, S. K. 2016. Architecture of retinal projections to the central circadian pacemaker. *Proc Natl Acad Sci U S A,* 113**,** 6047-52.

FERNANDEZ, D. C., FOGERSON, P. M., LAZZERINI OSPRI, L., THOMSEN, M. B., LAYNE, R. M., SEVERIN, D., ZHAN, J., SINGER, J. H., KIRKWOOD, A., ZHAO, H., BERSON, D. M. & HATTAR,

S. 2018. Light Affects Mood and Learning through Distinct Retina-Brain Pathways. *Cell,* 175**,** 71-84.e18.

FREMEAU, R. T., JR., TROYER, M. D., PAHNER, I., NYGAARD, G. O., TRAN, C. H., REIMER, R. J., BELLOCCHIO, E. E., FORTIN, D., STORM-MATHISEN, J. & EDWARDS, R. H. 2001. The expression of vesicular glutamate transporters defines two classes of excitatory synapse. *Neuron,* 31**,** 247-60.

FU, Y. & YAU, K. W. 2007. Phototransduction in mouse rods and cones. *Pflugers Arch,* 454**,** 805-19.

FU, Y., ZHONG, H., WANG, M. H., LUO, D. G., LIAO, H. W., MAEDA, H., HATTAR, S., FRISHMAN, L. J. & YAU, K. W. 2005. Intrinsically photosensitive retinal ganglion cells detect light with a vitamin A-based photopigment, melanopsin. *Proc Natl Acad Sci U S A,* 102**,** 10339-44.

GALL, A. J. & SHUBONI-MULLIGAN, D. D. 2022. Keep Your Mask On: The Benefits of Masking for Behavior and the Contributions of Aging and Disease on Dysfunctional Masking Pathways. *Front Neurosci,* 16**,** 911153.

GIRARDET, C., BLANCHARD, M. P., FERRACCI, G., LÉVÊQUE, C., MORENO, M., FRANÇOIS-BELLAN, A. M., BECQUET, D. & BOSLER, O. 2010. Daily changes in synaptic innervation of VIP neurons in the rat suprachiasmatic nucleus: contribution of glutamatergic afferents. *Eur J Neurosci,* 31**,** 359-70.

GIZOWSKI, C., ZAELZER, C. & BOURQUE, C. W. 2016. Clock-driven vasopressin neurotransmission mediates anticipatory thirst prior to sleep. *Nature,* 537**,** 685-8.

GOMPF, H. S., FULLER, P. M., HATTAR, S., SAPER, C. B. & LU, J. 2015. Impaired circadian photosensitivity in mice lacking glutamate transmission from retinal melanopsin cells. *J Biol Rhythms,* 30**,** 35-41.

GOURSAUD, S., MALOTEAUX, J. M. & HERMANS, E. 2008. Activation of VIP/PACAP type 2 receptor by the peptide histidine isoleucine in astrocytes influences GLAST-mediated glutamate uptake. *J Neurochem,* 105**,** 1165-75.

GUNDELFINGER, E. D., KESSELS, M. M. & QUALMANN, B. 2003. Temporal and spatial coordination of exocytosis and endocytosis. *Nat Rev Mol Cell Biol,* 4**,** 127-39.

HAMNETT, R., CROSBY, P., CHESHAM, J. E. & HASTINGS, M. H. 2019. Vasoactive intestinal peptide controls the suprachiasmatic circadian clock network via ERK1/2 and DUSP4 signalling. *Nature Communications,* 10**,** 542.

HANNIBAL, J. 2002. Neurotransmitters of the retino-hypothalamic tract. *Cell Tissue Res,* 309**,** 73-88.

HANNIBAL, J., DING, J. M., CHEN, D., FAHRENKRUG, J., LARSEN, P. J., GILLETTE, M. U. & MIKKELSEN, J. D. 1997. Pituitary adenylate cyclase-activating peptide (PACAP) in the retinohypothalamic tract: a potential daytime regulator of the biological clock. *J Neurosci,* 17**,** 2637-44.

HANNIBAL, J., HINDERSSON, P., KNUDSEN, S. M., GEORG, B. & FAHRENKRUG, J. 2002. The photopigment melanopsin is exclusively present in pituitary adenylate cyclase-activating polypeptide-containing retinal ganglion cells of the retinohypothalamic tract. *J Neurosci,* 22**,** Rc191.

HANSEN, K. B., WOLLMUTH, L. P., BOWIE, D., FURUKAWA, H., MENNITI, F. S., SOBOLEVSKY, A. I., SWANSON, G. T., SWANGER, S. A., GREGER, I. H., NAKAGAWA, T., MCBAIN, C. J., JAYARAMAN, V., LOW, C. M., DELL'ACQUA, M. L., DIAMOND, J. S., CAMP, C. R., PERSZYK, R. E., YUAN, H. & TRAYNELIS, S. F. 2021. Structure, Function, and Pharmacology of Glutamate Receptor Ion Channels. *Pharmacol Rev,* 73**,** 298-487.

HARDELAND, R., CARDINALI, D. P., BROWN, G. M. & PANDI-PERUMAL, S. R. 2015. Melatonin and brain inflammaging. *Prog Neurobiol,* 127-128**,** 46-63.

HARMAR, A. J., MARSTON, H. M., SHEN, S., SPRATT, C., WEST, K. M., SHEWARD, W. J., MORRISON, C. F., DORIN, J. R., PIGGINS, H. D., REUBI, J. C., KELLY, J. S., MAYWOOD, E. S. & HASTINGS, M. H. 2002. The VPAC(2) receptor is essential for circadian function in the mouse suprachiasmatic nuclei. *Cell,* 109**,** 497-508.

HASTINGS, M. H., BRANCACCIO, M., GONZALEZ-APONTE, M. F. & HERZOG, E. D. 2023. Circadian Rhythms and Astrocytes: The Good, the Bad, and the Ugly. *Annu Rev Neurosci,* 46**,** 123-143.

HATTAR, S., LIAO, H. W., TAKAO, M., BERSON, D. M. & YAU, K. W. 2002. Melanopsin-containing retinal ganglion cells: architecture, projections, and intrinsic photosensitivity. *Science,* 295**,** 1065-70.

HAYASHI, M. K. 2018. Structure-Function Relationship of Transporters in the Glutamate-Glutamine Cycle of the Central Nervous System. *Int J Mol Sci,* 19.

HERDE, M. K., BOHMBACH, K., DOMINGOS, C., VANA, N., KOMOROWSKA-MÜLLER, J. A., PASSLICK, S., SCHWARZ, I., JACKSON, C. J., DIETRICH, D., SCHWARZ, M. K. & HENNEBERGER, C. 2020. Local Efficacy of Glutamate Uptake Decreases with Synapse Size. *Cell Rep,* 32**,** 108182.

HU, C., HILL, D. D. & WONG, K. Y. 2013. Intrinsic physiological properties of the five types of mouse ganglion-cell photoreceptors. *J Neurophysiol,* 109**,** 1876-89.

IZUMO, M., PEJCHAL, M., SCHOOK, A. C., LANGE, R. P., WALISSER, J. A., SATO, T. R., WANG, X., BRADFIELD, C. A. & TAKAHASHI, J. S. 2014. Differential effects of light and feeding on circadian organization of peripheral clocks in a forebrain Bmal1 mutant. *Elife,* 3.

JOHNSON, J. 2007. Vesicular Glutamate Transporter 1 Is Required for Photoreceptor Synaptic Signaling But Not For Intrinsic Visual Functions.

JOHNSON, J., FREMEAU, R. T., JR., DUNCAN, J. L., RENTERÍA, R. C., YANG, H., HUA, Z., LIU, X., LAVAIL, M. M., EDWARDS, R. H. & COPENHAGEN, D. R. 2007. Vesicular glutamate transporter 1 is required for photoreceptor synaptic signaling but not for intrinsic visual functions. *J Neurosci,* 27**,** 7245-55.

JOHNSON, R. F., MORIN, L. P. & MOORE, R. Y. 1988. Retinohypothalamic projections in the hamster and rat demonstrated using cholera toxin. *Brain Res,* 462**,** 301-12.

JONES, J. R., SIMON, T., LONES, L. & HERZOG, E. D. 2018. SCN VIP Neurons Are Essential for Normal Light-Mediated Resetting of the Circadian System. *J Neurosci,* 38**,** 7986-7995.

KAESER, P. S. & REGEHR, W. G. 2017. The readily releasable pool of synaptic vesicles. *Curr Opin Neurobiol,* 43**,** 63-70.

KALSBEEK, A., LA FLEUR, S. & FLIERS, E. 2014. Circadian control of glucose metabolism. *Mol Metab,* 3**,** 372-83.

KALSBEEK, A., PALM, I. F., LA FLEUR, S. E., SCHEER, F. A. J. L., PERREAU-LENZ, S., RUITER, M., KREIER, F., CAILOTTO, C. & BUIJS, R. M. 2006. SCN Outputs and the Hypothalamic Balance of Life. *Journal of Biological Rhythms,* 21**,** 458-469.

KHAPRE, R. V., KONDRATOVA, A. A., PATEL, S., DUBROVSKY, Y., WROBEL, M., ANTOCH, M. P. & KONDRATOV, R. V. 2014. BMAL1-dependent regulation of the mTOR signaling pathway delays aging. *Aging (Albany NY),* 6**,** 48-57.

KIM, K. Y., RIOS, L. C., LE, H., PEREZ, A. J., PHAN, S., BUSHONG, E. A., DEERINCK, T. J., LIU, Y. H., ELLISMAN, M. A., LEV-RAM, V., JU, S., PANDA, S. A., YOON, S., HIRAYAMA, M., MURE, L. S., HATORI, M., ELLISMAN, M. H. & PANDA, S. 2019. Synaptic Specializations of Melanopsin-Retinal Ganglion Cells in Multiple Brain Regions Revealed by Genetic Label for Light and Electron Microscopy. *Cell Rep,* 29**,** 628-644.e6.

KISS, J., HALÁSZ, B., CSÁKI, A., LIPOSITS, Z. & HRABOVSZKY, E. 2007. Vesicular glutamate transporter 2 protein and mRNA containing neurons in the hypothalamic suprachiasmatic nucleus of the rat. *Brain Res Bull,* 74**,** 397-405.

KONDRATOV, R. V., KONDRATOVA, A. A., GORBACHEVA, V. Y., VYKHOVANETS, O. V. & ANTOCH, M. P. 2006. Early aging and age-related pathologies in mice deficient in BMAL1, the core componentof the circadian clock. *Genes Dev,* 20**,** 1868-73.

KONDRATOVA, A. A., DUBROVSKY, Y. V., ANTOCH, M. P. & KONDRATOV, R. V. 2010. Circadian clock proteins control adaptation to novel environment and memory formation. *Aging (Albany NY),* 2**,** 285-97.

KORF, H.-W. & VON GALL, C. 2013. Circadian Physiology. *Neuroscience in the 21st Century.*

KORF, H. W. & VON GALL, C. 2006. Mice, melatonin and the circadian system. *Mol Cell Endocrinol,* 252**,** 57-68.

KORF, H. W. & VON GALL, C. 2024. Mouse Models in Circadian Rhythm and Melatonin Research. *J Pineal Res,* 76**,** e12986.

KUMAR, D., KHAN, B., OKCAY, Y., SIS, Ç. Ö., ABDALLAH, A., MURRAY, F., SHARMA, A., UEMURA, M., TALIYAN, R., HEINBOCKEL, T., RAHMAN, S. & GOYAL, R. 2024. Dynamic endocannabinoid-mediated neuromodulation of retinal circadian circuitry. *Ageing Research Reviews,* 99**,** 102401.

LAND, P. W., KYONKA, E. & SHAMALLA-HANNAH, L. 2004. Vesicular glutamate transporters in the lateral geniculate nucleus: expression of VGLUT2 by retinal terminals. *Brain Res,* 996**,** 251-4.

LEGATES, T. A., FERNANDEZ, D. C. & HATTAR, S. 2014. Light as a central modulator of circadian rhythms, sleep and affect. *Nat Rev Neurosci,* 15**,** 443-54.

LEONE, M. J., BEAULE, C., MARPEGAN, L., SIMON, T., HERZOG, E. D. & GOLOMBEK, D. A. 2015. Glial and light-dependent glutamate metabolism in the suprachiasmatic nuclei. *Chronobiol Int,* 32**,** 573-8.

LIGUZ-LECZNAR, M. & SKANGIEL-KRAMSKA, J. 2007. Vesicular glutamate transporters (VGLUTs): the three musketeers of glutamatergic system. *Acta Neurobiol Exp (Wars),* 67**,** 207-18.

MAO, W., GE, X., CHEN, Q. & LI, J.-D. 2025. Epigenetic Mechanisms in the Transcriptional Regulation of Circadian Rhythm in Mammals. *Biology,* 14**,** 42.

MCCAULEY, J. P., PETROCCIONE, M. A., D'BRANT, L. Y., TODD, G. C., AFFINNIH, N., WISNOSKI, J. J., ZAHID, S., SHREE, S., SOUSA, A. A., DE GUZMAN, R. M., MIGLIORE, R., BRAZHE, A., LEAPMAN, R. D., KHMALADZE, A., SEMYANOV, A., ZULOAGA, D. G., MIGLIORE, M. & SCIMEMI, A. 2020. Circadian Modulation of Neurons and Astrocytes Controls Synaptic Plasticity in Hippocampal Area CA1. *Cell Rep,* 33**,** 108255.

MÉNARD, C., QUIRION, R., VIGNEAULT, E., BOUCHARD, S., FERLAND, G., EL MESTIKAWY, S. & GAUDREAU, P. 2015. Glutamate presynaptic vesicular transporter and postsynaptic receptor levels correlate with spatial memory status in aging rat models. *Neurobiology of Aging,* 36**,** 1471-1482.

MIKKELSEN, J. D. & VRANG, N. 1994. A direct pretectosuprachiasmatic projection in the rat. *Neuroscience,* 62**,** 497-505.

MOORE, R. Y. 1997. Circadian rhythms: basic neurobiology and clinical applications. *Annu Rev Med,* 48**,** 253-66.

MOORE, R. Y., SPEH, J. C. & CARD, J. P. 1995. The retinohypothalamic tract originates from a distinct subset of retinal ganglion cells. *J Comp Neurol,* 352**,** 351-66.

MORIN, L. P. 1994. The circadian visual system. *Brain Research Reviews,* 19**,** 102-127.

MORIN, L. P. 2013. Neuroanatomy of the extended circadian rhythm system. *Exp Neurol,* 243**,** 4-20.

MROSOVSKY, N. 1999. Masking: history, definitions, and measurement. *Chronobiol Int,* 16**,** 415-29.

MROSOVSKY, N., SALMON, P. A., FOSTER, R. G. & MCCALL, M. A. 2000. Responses to light after retinal degeneration. *Vision Res,* 40**,** 575-8.

MUSIEK, E. S., LIM, M. M., YANG, G., BAUER, A. Q., QI, L., LEE, Y., ROH, J. H., ORTIZ-GONZALEZ, X., DEARBORN, J. T., CULVER, J. P., HERZOG, E. D., HOGENESCH, J. B., WOZNIAK, D. F., DIKRANIAN, K., GIASSON, B. I., WEAVER, D. R., HOLTZMAN, D. M. & FITZGERALD, G. A. 2013. Circadian clock proteins regulate neuronal redox homeostasis and neurodegeneration. *J Clin Invest,* 123**,** 5389-400.

NANCLARES, C., BARAIBAR, A. M., ARAQUE, A. & KOFUJI, P. 2021. Dysregulation of Astrocyte–Neuronal Communication in Alzheimer's Disease. *International Journal of Molecular Sciences,* 22**,** 7887.

OMOTE, H., MIYAJI, T., JUGE, N. & MORIYAMA, Y. 2011. Vesicular neurotransmitter transporter: bioenergetics and regulation of glutamate transport. *Biochemistry,* 50**,** 5558-65.

ONO, D., HONMA, K. I. & HONMA, S. 2021. Roles of Neuropeptides, VIP and AVP, in the Mammalian Central Circadian Clock. *Front Neurosci,* 15**,** 650154.

PARTCH, C. L., GREEN, C. B. & TAKAHASHI, J. S. 2014. Molecular architecture of the mammalian circadian clock. *Trends Cell Biol,* 24**,** 90-9.

PFEFFER, M., KORF, H. W. & VON GALL, C. 2015. Chronotype and stability of spontaneous locomotor activity rhythm in BMAL1-deficient mice. *Chronobiol Int,* 32**,** 81-91.

PFEFFER, M., MÜLLER, C. M., MORDEL, J., MEISSL, H., ANSARI, N., DELLER, T., KORF, H. W. & VON GALL, C. 2009. The mammalian molecular clockwork controls rhythmic expression of its own input pathway components. *J Neurosci,* 29**,** 6114-23.

PFEFFER, M., ZIMMERMANN, Z., GISPERT, S., AUBURGER, G., KORF, H. W. & VON GALL, C. 2018. Impaired Photic Entrainment of Spontaneous Locomotor Activity in Mice Overexpressing Human Mutant α-Synuclein. *Int J Mol Sci,* 19.

PICKARD, G. E. 1985. Bifurcating axons of retinal ganglion cells terminate in the hypothalamic suprachiasmatic nucleus and the intergeniculate leaflet of the thalamus. *Neurosci Lett,* 55**,** 211-7.

PICKARD, G. E. & SOLLARS, P. J. 2012. Intrinsically photosensitive retinal ganglion cells. *Rev Physiol Biochem Pharmacol,* 162**,** 59-90.

PURRIER, N., ENGELAND, W. C. & KOFUJI, P. 2014. Mice deficient of glutamatergic signaling from intrinsically photosensitive retinal ganglion cells exhibit abnormal circadian photoentrainment. *PLoS One,* 9**,** e111449.

REDLIN, U., HATTAR, S. & MROSOVSKY, N. 2005. The circadian Clock mutant mouse: impaired masking response to light. *J Comp Physiol A Neuroethol Sens Neural Behav Physiol,* 191**,** 51-9.

REGHUNANDANAN, V. 2024. Functional interactions between neurotransmitters and neuropeptides in regulating suprachiasmatic nucleus function and circadian rhythms. *Exploration of Neuroscience,* 3**,** 434-477.

REGHUNANDANAN, V. & REGHUNANDANAN, R. 2006. Neurotransmitters of the suprachiasmatic nuclei. *J Circadian Rhythms,* 4**,** 2.

REINER, A. & LEVITZ, J. 2018. Glutamatergic Signaling in the Central Nervous System: Ionotropic and Metabotropic Receptors in Concert. *Neuron,* 98**,** 1080-1098.

REPPERT, S. M. & WEAVER, D. R. 2002. Coordination of circadian timing in mammals. *Nature,* 418**,** 935-941.

RICCITELLI, S., BOI, F., LONARDONI, D., GIANTOMASI, L., BARCA-MAYO, O., DE PIETRI TONELLI, D., BISTI, S., DI MARCO, S. & BERDONDINI, L. 2022. Glial Bmal1 role in mammalian retina daily changes. *Sci Rep,* 12**,** 21561.

ROJO, D., BADNER, A., DAL CENGIO, L., KIM, S., SAKAI, N., GREENE, J., EISINGER, E., ARELLANO-GARCIA, C., MEHL, L. C., GUMMA, M. E., SOYK, R. L., RANSOM, J., WEIGEL, M. K., YALÇıN, B., JONES, S. E., OLLILA, H. M., NISHINO, S. & GIBSON, E. M. 2022. BMAL1 loss in oligodendroglial lineage cells dysregulates myelination and sleep. *bioRxiv***,** 2022.04.28.489946.

ROSENMUND, C. & STEVENS, C. F. 1996. Definition of the readily releasable pool of vesicles at hippocampal synapses. *Neuron,* 16**,** 1197-207.

SAMSA, W. E., VASANJI, A., MIDURA, R. J. & KONDRATOV, R. V. 2016. Deficiency of circadian clock protein BMAL1 in mice results in a low bone mass phenotype. *Bone,* 84**,** 194-203.

SCHMIDT, T. M., CHEN, S. K. & HATTAR, S. 2011a. Intrinsically photosensitive retinal ganglion cells: many subtypes, diverse functions. *Trends Neurosci,* 34**,** 572-80.

SCHMIDT, T. M., DO, M. T., DACEY, D., LUCAS, R., HATTAR, S. & MATYNIA, A. 2011b. Melanopsin-positive intrinsically photosensitive retinal ganglion cells: from form to function. *J Neurosci,* 31**,** 16094-101.

SCHMIDT, T. M. & KOFUJI, P. 2009. Functional and morphological differences among intrinsically photosensitive retinal ganglion cells. *J Neurosci,* 29**,** 476-82.

SCHMIDT, T. M. & KOFUJI, P. 2011. Structure and function of bistratified intrinsically photosensitive retinal ganglion cells in the mouse. *J Comp Neurol,* 519**,** 1492-504.

SEGOVIA, G., PORRAS, A., DEL ARCO, A. & MORA, F. 2001. Glutamatergic neurotransmission in aging: a critical perspective. *Mechanisms of Ageing and Development,* 122**,** 1-29.

ŠERÝ, O., SULTANA, N., KASHEM, M. A., POW, D. V. & BALCAR, V. J. 2015. GLAST But Not Least--Distribution, Function, Genetics and Epigenetics of L-Glutamate Transport in Brain--Focus on GLAST/EAAT1. *Neurochem Res,* 40**,** 2461-72.

SHINOHARA, K., HONMA, S., KATSUNO, Y., ABE, H. & HONMA, K.-I. 1994. Circadian rhythms in the release of vasoactive intestinal polypeptide and arginine-vasopressin in organotypic slice culture of rat suprachiasmatic nucleus. *Neuroscience Letters,* 170**,** 183-186.

SILVEIRA, E. J. D., NASCIMENTO FILHO, C. H. V., YUJRA, V. Q., WEBBER, L. P., CASTILHO, R. M. & SQUARIZE, C. H. 2020. BMAL1 Modulates Epidermal Healing in a Process Involving the Antioxidative Defense Mechanism. *Int J Mol Sci,* 21.

SILVER, R. & KRIEGSFELD, L. J. 2014. Circadian rhythms have broad implications for understanding brain and behavior. *Eur J Neurosci,* 39**,** 1866-80.

SPANAGEL, R., PENDYALA, G., ABARCA, C., ZGHOUL, T., SANCHIS-SEGURA, C., MAGNONE, M. C., LASCORZ, J., DEPNER, M., HOLZBERG, D., SOYKA, M., SCHREIBER, S., MATSUDA, F., LATHROP, M., SCHUMANN, G. & ALBRECHT, U. 2005. The clock gene Per2 influences the glutamatergic system and modulates alcohol consumption. *Nat Med,* 11**,** 35-42.

STORCH, K. F., PAZ, C., SIGNOROVITCH, J., RAVIOLA, E., PAWLYK, B., LI, T. & WEITZ, C. J. 2007. Intrinsic circadian clock of the mammalian retina: importance for retinal processing of visual information. *Cell,* 130**,** 730-741.

TASKER, J. G. & HERMAN, J. P. 2011. Mechanisms of rapid glucocorticoid feedback inhibition of the hypothalamic-pituitary-adrenal axis. *Stress,* 14**,** 398-406.

TELEANU, R. I., NICULESCU, A. G., ROZA, E., VLADÂCENCO, O., GRUMEZESCU, A. M. & TELEANU, D. M. 2022. Neurotransmitters-Key Factors in Neurological and Neurodegenerative Disorders of the Central Nervous System. *Int J Mol Sci,* 23.

THOMPSON, S., PHILP, A. R. & STONE, E. M. 2008. Visual function testing: a quantifiable visually guided behavior in mice. *Vision Res,* 48**,** 346-52.

TODD, A. C. & HARDINGHAM, G. E. 2020. The Regulation of Astrocytic Glutamate Transporters in Health and Neurodegenerative Diseases. *Int J Mol Sci,* 21.

VINDLACHERUVU, R. R., EBLING, F. J., MAYWOOD, E. S. & HASTINGS, M. H. 1992. Blockade of Glutamatergic Neurotransmission in the Suprachiasmatic Nucleus Prevents Cellular and Behavioural Responses of the Circadian System to Light. *Eur J Neurosci,* 4**,** 673-679.

VITATERNA, M. H., TAKAHASHI, J. S. & TUREK, F. W. 2001. Overview of circadian rhythms. *Alcohol Res Health,* 25**,** 85-93.

VON GALL, C. 2022. The Effects of Light and the Circadian System on Rhythmic Brain Function. *Int J Mol Sci,* 23.

VON GALL, C., STEHLE, J. H. & WEAVER, D. R. 2002. Mammalian melatonin receptors: molecular biology and signal transduction. *Cell Tissue Res,* 309**,** 151-62.

WELSH, D. K., TAKAHASHI, J. S. & KAY, S. A. 2010. Suprachiasmatic nucleus: cell autonomy and network properties. *Annu Rev Physiol,* 72**,** 551-77.

WINTER, H. C. & UEDA, T. 2008. The glutamate uptake system in presynaptic vesicles: further characterization of structural requirements for inhibitors and substrates. *Neurochem Res,* 33**,** 223-31.

YANG, G., CHEN, L., ZHANG, J., REN, B. & FITZGERALD, G. A. 2019. Bmal1 deletion in mice facilitates adaptation to disrupted light/dark conditions. *JCI Insight,* 5.

YASSINE, M., HASSAN, S. A., YÜCEL, L. A., PURATH, F. F. A., KORF, H.-W., VON GALL, C. & ALI, A. A. H. 2024. Hepatocellular Carcinoma in Mice Affects Neuronal Activity and Glia Cells in the Suprachiasmatic Nucleus. *Biomedicines,* 12**,** 2202.

YELAMANCHILI, S. V., PENDYALA, G., BRUNK, I., DARNA, M., ALBRECHT, U. & AHNERT-HILGER, G. 2006. Differential sorting of the vesicular glutamate transporter 1 into a defined

vesicular pool is regulated by light signaling involving the clock gene Period2. *J Biol Chem,* 281**,** 15671-9.

ZHOU, Y. & DANBOLT, N. C. 2014. Glutamate as a neurotransmitter in the healthy brain. *Journal of Neural Transmission,* 121**,** 799-817.

Danksagung

Ich möchte mich insbesondere bei meiner Doktormutter, Frau Professorin Dr. von Gall, bedanken. Sowohl im Rahmen des Studiums, als meine Dozentin in der Neuroanatomie und Tischdozentin in der anatomischen Präparation, als auch im Rahmen meiner Rolle als Doktorand in Ihrem angesehenen Institut hatte ich die Gelegenheit, meine Begeisterung für die Anatomie, insbesondere die Neuroanatomie, auszuleben. Sie ist eine weltoffene und tolerante Professorin, die sehr viel Liebe in sich trägt und stets nur das Beste für Ihre Studenten möchte, sie fördert und in ihrer Weiterentwicklung unterstützt. Insbesondere mir als Arbeiterkind mit Migrationshintergrund hat Sie die Gelegenheit gegeben, ein Interessantes Projekt mitzugestalten und mir die Welt der Wissenschaft eröffnet. Als Student durfte ich Sie zum EBRS Kongress in Lyon begleiten, wo ich die Gelegenheit hatte, internationale Forscher kennenzulernen, die ich in persönlich traf und teilweise in meiner Doktorarbeit zitiert habe. Ich wünsche Professorin Dr. von Gall Gesundheit, Zufriedenheit sowie weiterhin viel Erfolg in Ihrer Lehre und Forschung.

Eine weitere zentrale Person im Rahmen meiner Doktorarbeit und später auch als persönliche Bezugsperson und mittlerweile sogar als gute Freundin, ist Frau Dr. Amira Ali. Ich könnte mir keine bessere Mitautorin vorstellen als Sie. Ich habe sehr lange an dieser Doktorarbeit gearbeitet und Frau Dr. Amira Ali, hatte immer ein offenes Ohr für meine Sorgen, Zweifel und auch privaten Belange. Ihre Rolle als Mentorin, gemeinsam mit Frau Professorin Dr. von Gall, hat mir geholfen diesen beschwerlichen Weg erfolgreich und mit Freude zu bewältigen.

Ohne die Hilfe des gesamten labortechnischen Teams, sprich Angelika Hallenberger, Ulla Lammersen, Hanna Bellert und Ralf Faßbender, hätte ich nicht so eine hervorragende wissenschaftliche Arbeitsweise erlernen dürfen. Die Einführung und Anleitung in den Versuchsaufbau und die Durchführung waren auf höchstem Niveau, und Ihre Unterstützung war von großer Bedeutung für den Erfolg dieser Doktorarbeit.

Ein weiterer Dank gilt den Wissenschaftlichen Mitarbeitenden im Institut, die mir sowohl im Rahmen der zahlreichen Labmeetings als auch bei meinen Zwischenberichten und Präsentationen kritisch und mit wertvollen Verbesserungsvorschläge zur Seite standen.

Ich möchte mich bei Hussein Haidar, Jane K. Schröder, Johanna Hallenberger und Ahmed Sami Saher Al-Chalabi für ihre Unterstützung bedanken.

Vielen Dank, liebe Frau Verena Lehmkuhl, ich kann mich an keinen Tag erinnern, an dem du nicht freundlich und hilfsbereit warst.

Ich möchte mich darüber hinaus bei meinen beiden Eltern bedanken. Sie haben mich stets unterstützt und bestärkt, den akademischen Weg zu gehen, und mich nach Kräften gefördert. Meine beiden Geschwister, Hasan und Büsra Korkmaz, haben meine Zweifel immer wieder bereinigt und mich motiviert, diesen Weg bis zum Schluss zu gehen.

Darüber hinaus möchte ich mich bei meinen beiden Freunden, Hanibaal Dib und Burak Korkmazcan bedanken, die mir während der Doktorarbeit und des gesamten Medizinstudiums motivierend zur Seite standen.